

Remote Paleohydrograph Reconstruction of the Stockton Island Tombolo

by

Dayna Ann Opersko

Supervised by: Dr. John Johnston

A thesis

Presented to the University Of Waterloo

In fulfilment of the

Thesis requirement for the degree of

Honours Bachelor of Science

In Earth Science

Waterloo, Ontario, Canada

© Dayna A. Opersko, 2021

Author's Declaration

I hereby declare that I am the sole author of this thesis. This is a true copy of the thesis, including any required final revisions, as accepted by my examiners.

I understand that my thesis may be made electronically available to the public.

Dayna Ann Opersko

Abstract

Rising lake levels have become a concern for the coasts of Lake Superior and one such coastline is the Stockton Island Tombolo (SIT) that protects the Pine Barrens Habitat (PBH) in the Apostle Islands National Lakeshore (AINL), Wisconsin, United States of America. If the SIT is lost, the threatened and endangered species that live within the PBH will disappear. For the AINL managers to make an informed decision on how to protect this unique and sensitive area, they need to understand how lake level and coastal sediments will change. Lake level trends and patterns for Lake Superior have been reconstructed from ancient, preserved shorelines, creating paleohydrographs that help to understand how lake level has changed in the past by comparing age and elevation (Johnston et al., 2012). Though fieldwork has been postponed due to COVID-19, there is an opportunity here to develop ideas mentioned in Johnston et al. (2012) and Heather (2021) using topographic elevations and a correction factor to reconstruct a paleohydrograph from the ancient shorelines at AINL. Elevations were retrieved from light detection and ranging (LIDAR) data, afterwards a Digital Elevation Model (DEM) was created. The DEM was divided into the East and West strandplains and one transect from each was chosen then the two were combined to represent one SIT pattern. Then elevations were adjusted to estimate the base of the foreshore contact, normally obtained from coring shorelines to interpret past lake level elevations. Trends and patterns in the representative paleohydrograph are then compared to paleohydrographs from Johnston et al. (2012) to determine approximate ages for the ridges in the SIT. The more landward ridges, are determined to be from the Nipissing phase while the lakeward ridges, are from the Sub-Sault phase. This new remote paleohydrograph reconstruction for SIT helps to preliminarily interpret strandplain sequences on the SIT and will potentially help guide future fieldwork and better understand the context for managing the SIT and PBH in AINL.

Acknowledgement

I would like to thank Dr. John Johnston, my thesis advisor, for his insight, guidance, and expertise throughout the process as well as his valuable editing of my thesis. It has truly been an honour working on this thesis with you.

Marcel Heather for providing me the results of his thesis and the method he has developed.

Emily Secord for her help editing and her support throughout this process.

Sterling Whittaker-Hawkins for his help editing this thesis.

Markus Wieland from the University of Waterloo Geospatial Centre for answering questions and helping me through using ArcGIS to produce maps from LIDAR data.

Kate Mercer from the University of Waterloo Library for her assistance in finding resources and literature for this thesis.

My family for their support and encouragement they have given to me throughout this process.

Table of Contents

1.0 Introduction.....	1
2.0 Background.....	4
2.1 Apostle Islands National Lakeshore (AINL)	4
2.1.1 Surficial Geology.....	4
2.1.2 Pine Barrens Habitat.....	5
2.1.3 Coastal Change.....	5
2.2 Coastal Landscapes	7
2.2.1 Beaches.....	8
2.2.2 Strandplains	9
2.2.3 Spits and Tombolos	9
2.3 Paleohydrographic Research.....	10
2.3.1 Water Level Important Dates	11
2.3.2 Paleohydrograph Reconstruction through Fieldwork.....	11
2.3.3 Paleohydrograph Reconstruction Through Topography	12
2.4 Topographic Elevation - LIDAR	13
2.5 Glacial Isostatic Adjustment	14
2.5.1 Calculating GIA Using Lake-Level Gauge Data.....	14
2.5.2 Calculating GIA Using Paleohydrographs	15
2.6 Summary	16
3.0 Goals and Objectives	17
4.0 Experimental Design and Methods.....	18
4.1 Collecting Data.....	18
4.2 Creating the Digital Elevation Model	19
4.3 Deriving Data from Transects.....	22
4.4 Excel Datasets and Graphs.....	23
5.0 Results and Discussion	25
5.1 Raw LIDAR Data.....	25
5.2 Digital Elevation Model.....	29
5.3 Topographic Transects.....	33
5.4 Excel Data	34
5.5 Selecting and Adjusting Topographic Elevation.....	39
5.6 Common Discontinuity in the Lake Superior Strandplains	43

5.7 Determining Discontinuities Within the Strandplain Data	47
5.8 Representative Stockton Island Tombolo Elevation Pattern.....	48
5.9 Determination of Potential Age	49
5.10 Age Determination Using the Sault Ste. Marie Outlet Paleohydrograph	53
5.11 Validity of the Method.....	61
5.12 Sources of Error	62
5.13 Erosion and Flooding of the Stockton Island Tombolo	63
6.0 Recommendations.....	65
7.0 Conclusion	66
8.0 References.....	68
Appendix A.....	70

List of Figures

Figure 1 Location of Apostle Islands National Lakeshore	2
Figure 2 Stockton Island Tombolo	2
Figure 3 Relative coastal change potential index of Apostle Islands National Lakeshore	6
Figure 4 Water level change in the Great Lakes	7
Figure 5 Diagram of a coast with the shore showing the development of a beach.....	8
Figure 6 Third generation model created from historic water-level data	15
Figure 7 Extent of the Stockton Island Tombolo and location of ridges	20
Figure 8 Distribution of the LAS files prior to being combined	26
Figure 9 LIDAR dataset created from combining the four LAS files	27
Figure 10 LIDAR dataset ground points layer	28
Figure 11 Extent of the Stockton Island Tombolo and its strandplains	30
Figure 12 Location of ridges in the East and West strandplains	32
Figure 13 Locations of transects for both the East and West strandplains	34
Figure 14 a-b Topographic elevation derived from the LIDAR DEM versus distance inland of the strandplain transects	35
Figure 14 c-e Topographic elevation derived from the LIDAR DEM versus distance inland of the strandplain transects.....	36
Figure 14 f Topographic elevation derived from the LIDAR DEM versus distance inland of the strandplain transects.....	37
Figure 15 Comparison of the West and East strandplains with derived elevation for the base of the foreshore contact and distance landward	42
Figure 16 Comparison of the elevations for the base of the foreshore contact and topographic LIDAR	42
Figure 17 Change of paleohydrograph slope based on the rate of glacial isostatic adjustment ...	46

Figure 18 Adjusted distances of the elevations for the base of the foreshore contact of the East and West Strandplains	48
Figure 19 Comparison of the Stockton Island Tombolo paleohydrograph pattern to previously reconstructed paleohydrograph patterns by distance landward	50
Figure 20 Glacial isostatic adjustment derived from water-level gauge data with previously reconstructed paleohydrograph study locations	51
Figure 21 Geomorphic evidence on the Stockton Island Tombolo supporting age estimate of lakeward ridges	52
Figure 22 Glacial isostatic rebound adjusted Sault Ste. Marie paleohydrograph compared to the Stockton Island Tombolo pattern	56
Figure 23 Glacial isostatic rebound adjusted Sault Ste. Marie paleohydrograph compared to the Stockton Island Tombolo pattern	57
Figure 24 Glacial isostatic rebound adjusted Sault Ste. Marie paleohydrograph compared to the Stockton Island Tombolo pattern	58

List of Tables

Table 1 Selections made to create the DEM.....	22
Table 2 Criteria to determine landward and lakeward sections of the East and West strandplain based on geomorphic characteristics	44
Table 3 Inferred ages determined by matching the inferred Stockton Island Tombolo paleohydrograph to the Sault Ste. Marie outlet paleohydrograph	60

List of Abbreviations

AINL	Apostle Islands National Lakeshore
BP	Before Present
DEM	Digital Elevation Model
GIA	Glacial Isostatic Adjustment
IGLD85	International Great Lakes Datum 1985
LIDAR	Light Detection and Ranging
NOAA	National Oceanic and Atmospheric Administration
NPS	National Park Service
OSL	Optically Stimulated Luminescence
PBH	Pine Barrens Habitat
SIT	Stockton Island Tombolo
SSM	Sault Ste. Marie
TNM	The National Map
U.S.A.	United States of America
USGS	United States Geological Survey

1.0 Introduction

In recent years relatively high-water levels have been experienced around the upper Great Lakes, which has contributed to increased coastal erosion and flooding. One location where land managers are concerned is in southwestern Lake Superior at Apostle Islands National Lakeshore (AINL), Wisconsin, United States of America (U.S.A.) (Figure 1). One area of concern for the AINL managers is the possible endangerment of an area known as the Pine Barrens Habitat (PBH) if water levels continue to rise since it is an ecosystem that has threatened and endangered flora and fauna (Thornberry-Ehrlich, 2015). The PBH is located on the Stockton Island Tombolo (SIT) that bridges two land masses, Stockton Island and Presque Isle, together with a sandscape known as a spit (Figure 2) (Thornberry-Ehrlich, 2015). The spit is composed of multiple beach ridges and is defined as a tombolo when it connects two islands (Owens, 1982). The National Park Service (NPS) has a mandate stating they must preserve and protect the natural environment to the best of their ability (National Park Service, 2011). Risk of erosion and flooding from lake-level rise was deemed to be a high risk to this area in Pendleton et al. (2007). Due to anticipated erosion and flooding of the SIT, the amount of lake level rise is yet to be studied and understanding how it will change can help make informed decisions at AINL. To determine the extremity of the endangerment to the SIT and PBH, park managers contacted a research group that has expertise studying natural lake-level changes and shoreline behaviour of the upper Great Lakes coastlines. Lake-level trends and patterns for Lake Superior have been reconstructed from ancient, preserved shorelines, creating paleohydrographs that help to understand how lake-levels have changed in the past using elevation and age data (Johnston et al., 2012). Understanding lake-level trends and patterns of the past and correlating them to the present trends and patterns allows for informed predictions of future lake-levels and thus erosion

and flooding can be estimated. Recognizing how relatively short-term rising and naturally short- and long-term oscillating lake-levels may affect the tombolo is important to understand the severity of erosion, working against the protection measure of the park for the PHB.



Figure 1 Location of Apostle Islands National Lakeshore. Location of Apostle Islands National Lakeshore (AINL), outlined by the red box, is within the Great Lakes along the southwestern coastline of Lake Superior in the state of Wisconsin, U.S.A.



Figure 2 Stockton Island Tombolo. Stockton Island Tombolo (SIT) connecting Stockton Island to Presque Isle located within Apostle Islands National Lakeshore. Evidence of flooding can be seen in the low-lying lagoons (elongated black areas) between elevated ancient shorelines (brown-coloured areas) on the eastern side of the SIT.

Unfortunately, due to the COVID-19 pandemic, research that was supposed to start in the summer of 2020 has been postponed, delaying the collection of data and subsequent research. Fortunately, there is a method that can be done, which allows for a paleohydrograph to be developed remotely by using topographic elevation data and a pre-existing paleohydrograph from a nearby study site first mentioned in Johnston et al. (2012) and further developed in Heather (2021). Although topographic elevation paleohydrograph reconstruction is recognized as a less accurate method compared to finding the subsurface sedimentary contact elevation through coring, the topographic elevation method can provide preliminary estimates before fieldwork is completed and may be applicable in remote areas for paleohydrograph reconstruction. The most accurate and detailed topographic elevations are retrieved using LIDAR data and in the Great Lakes from the National Oceanic and Atmospheric Administration (NOAA). However ancient shorelines move vertically overtime due to glacial isostatic adjustment (GIA), which is ongoing due to the long-gone Laurentide Icesheet that advanced and retreated across the Great Lakes (Johnston et al., 2014). When analyzing elevation data around the Great Lakes, it is very important to account for the small but persistent process of GIA. Creating a preliminary paleohydrograph for the SIT would better help the understanding of the SIT and PBH prior to the completion of fieldwork. Furthermore, it will potentially help make decisions on core locations and number of cores through ancient shorelines at SIT.

2.0 Background

2.1 Apostle Islands National Lakeshore (AINL)

Numerous studies have been completed at AINL, but the focus of these studies has mainly been on the flora and fauna, although some research has been conducted by the United States Geological Survey (USGS) on AINL. For this undergraduate thesis, the background of AINL is focused on the surficial geology of AINL, the Pine Barrens Habitat, and research about potential change to the modern coast.

2.1.1 Surficial Geology

The surficial geology of AINL has been mainly formed from glacial tills and sandscapes related to Lake Superior (Cary, McDowell, & Graumlich, 1979; Thornberry-Ehrlich, 2015). Till deposits are mainly found on the mainland and islands of the park while the sandscapes are formed around the shorelines (Cary et al., 1979; Thornberry-Ehrlich, 2015). Though there are many sandscapes that occur within AINL, the focus of this thesis is on tombolos. Tombolos often form in low-energy environments that allow for the settling and deposition of sediment out of the lake water and forms a sand spit that connects two islands (Thornberry-Ehrlich, 2015). For the SIT, it is composed of two tombolos which formed as one larger tombolo that now connects Stockton Island and Presque Isle together (Thornberry-Ehrlich, 2015). All soils within AINL have formed during the past 11,000 years during and after the retreat of the Laurentide Icesheet (Cary et al., 1979). Due to the nature of sandscapes which naturally experience erosion and deposition and change overtime, the AINL Management Plan avoids disrupting these natural processes (National Park Service, 2011).

2.1.2 Pine Barrens Habitat

The PBH is located on the SIT and is considered to be greatly at risk and of concern for the Wisconsin Department of Natural Resources, so more effort is placed on the preservation of this habitat (Huff, 2019). More specifically the PBH is located on the ridges of the ancient shorelines of the SIT where the soil is sandy and well-drained (Huff, 2019). Due to the confined range of the SIT and unique environment that it provides, the PBH would not find another suitable habitat upland to move to (Huff, 2019). Since the endangered flora and fauna present in this unique habitat and the NPS mandate to preserve and protect, if the PBH is deemed to be endangered from rising lake-levels, protection measures will have to be emplaced (National Park Service, 2011). Since the PBH occurs only on the SIT, the SIT must be protected to inevitably protect the PBH if rising lake-levels have a potential to flood and erode the SIT.

2.1.3 Coastal Change

Previous studies of the potential change of the shorelines within the AINL has been conducted by Pendleton et al. (2007). Through studying six different factors: geomorphology, historical shoreline change rate, regional coastal slope, relative sea-level change, mean significant wave height, and mean annual ice cover, allowed for a change potential index to be created (Pendleton et al., 2007). The SIT has a very high change potential index which is higher than the average index for AINL (Figure 3) (Pendleton et al., 2007). The very high change potential suggests that the PBH could be endangered if the change causes erosion or flooding of the SIT.

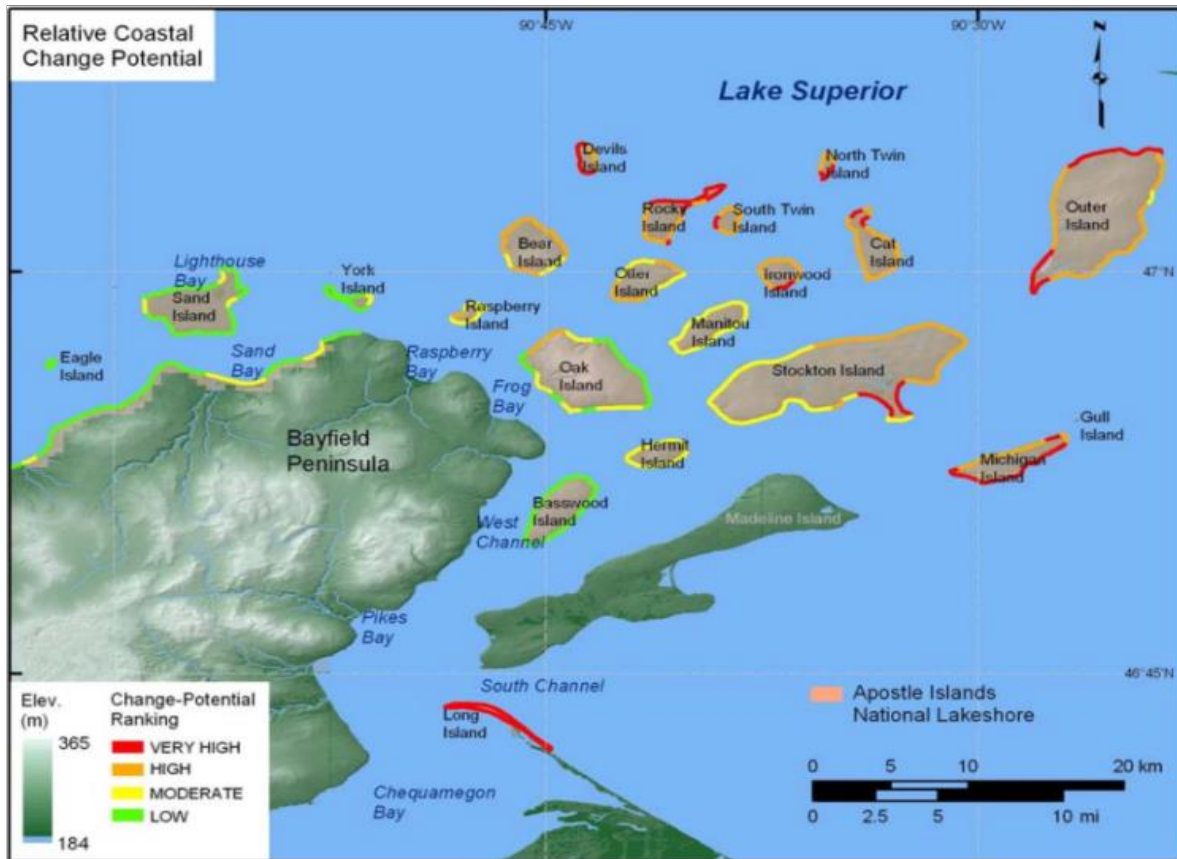


Figure 3 Relative coastal change potential index of Apostle Islands National Lakeshore. Relative change potential throughout the studied shorelines within AINL. The box indicates the location of the Stockton Island Tombolo that is listed as having a very high change potential. Adapted from (Pendleton et al., 2007).

In the past two decades Lake Superior has experienced lake level changes where it has been below and above the long-term average lake levels (Figure 4). Relatively low lake-levels occurred since 1999 and reached the lowest water level in the year 2007 but has recently experienced relatively high lake-levels (Figure 4) (United States Army Corps of Engineers [USACE], 2020). These recently high lake-levels show why the AINL managers are concerned about protecting both the SIT and PBH. To better understand how the SIT, a unique coastal feature, let us review general literature to create a conceptual model for the SIT and develop context of coastal landscapes relating to the SIT.

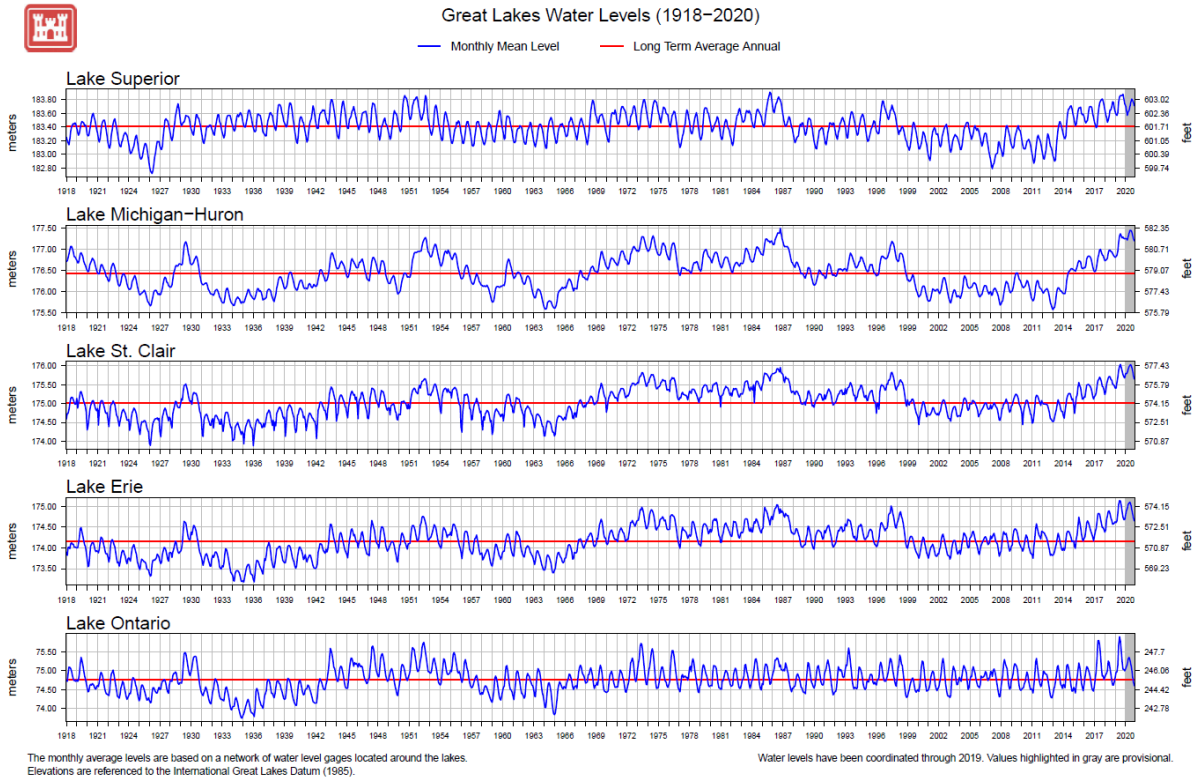


Figure 4 Water level change in the Great Lakes. For much of the early 2000's water levels were relatively low in Lake Superior compared to the long-term annual average with the levels in 2007 being the lowest in this century. Since 2013 the lake-levels began and continue to be high. Retrieved from (USACE, 2020).

2.2 Coastal Landscapes

Coastal landscapes develop between bodies of water such as, lakes or oceans, and land.

There are numerous types of coastal landscapes that form but this undergraduate thesis will focus on beaches and strandplains, as well as the coastal features of spits and tombolos. The coastline is a dynamic and complex environment and is the margin between land and water.

Coastlines are generally composed of two different types, erosional coastlines that have a relatively steeper gradient and depositional coastline, which have a shallower gradient (Nichols, 2009).

2.2.1 Beaches

Beaches form from waves and currents that deposit new sediment and erode existing material, and periodically rework the sediments mainly in the foreshore which may lead to the formation of a ridge known as a berm (Figure 5) (Nichols, 2009). When storm surges occur, the waves can exceed the top of the berm and into the backshore depositing sediment in a gradient that is shallower than the foreshore (Nichols, 2009). As shore progradation occurs, the beach will become protected by the new beach and aeolian deposits can accumulate on top of water-lain sediment (Otvos, 2017). This process is related to the theory of beach ridge formation in areas of coastline where deposited sediment is collected such as in embayments and may eventually create strandplains (Baedke and Thompson, 2000; Johnston et al., 2014; Otvos, 2017).

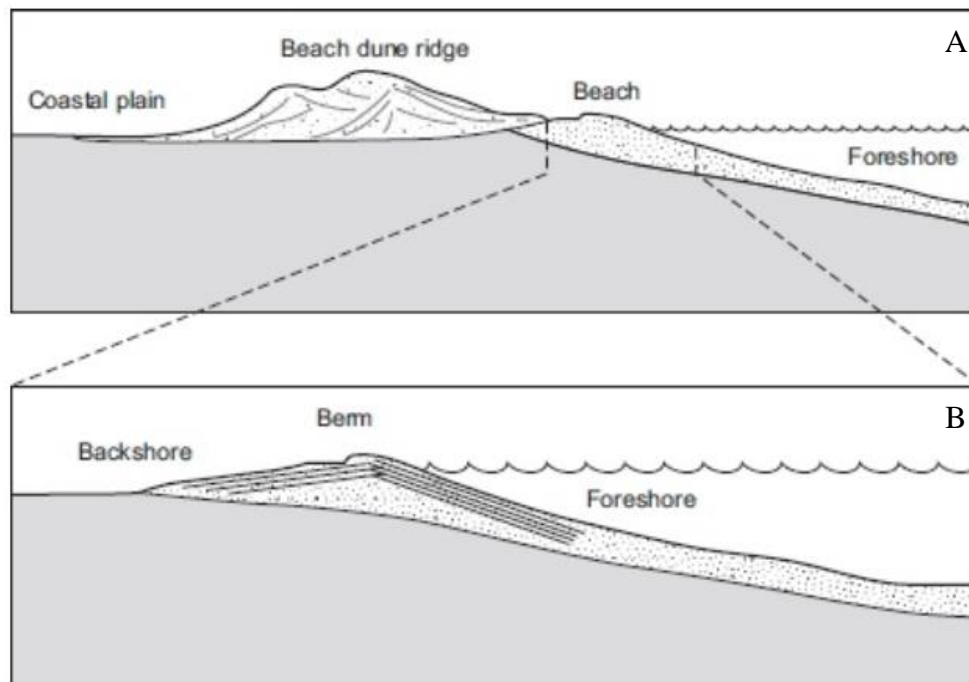


Figure 5 Diagram of a coast with the shore showing the development of a beach. A) Common coastline featuring beach dunes, and the beach representing the shore. B) Shore of the coast showing the locations of the backshore, berm, and foreshore. Retrieved from Nichols (2009).

2.2.2 Strandplains

Many ancient, preserved shorelines within an embayment are called strandplains. As the embayment fills up laterally, older ancient shorelines are protected from active coastal processes that occur along the shore, which causes erosion and deposition through wave activity (Nichols, 2009). Strandplains are composed of many laterally separated ancient beaches or ridges of sediment that are separated by swales, which can accumulate organics and sediments for wetlands to develop (Johnston et al., 2014). The older ridges and wetlands are protected from active processes on the beach since they are farther inland (Nichols, 2009). Strandplains can be described as progradational sequences or the building up of sediment which fill embayments causing them to become less arcuate as they fill with ridges (Nichols, 2009; Otvos, 2017). Formation and preservation of the late Holocene strandplains within the Great Lakes is due to two main factors: rate of water level change and rate of sediment supply (Johnston et al., 2007).

2.2.3 Spits and Tombolos

Spits are developed much like beaches and are defined as a sand barrier by Nichols (2009) since they are only partially attached to land with most of the spit surrounded by water. When a spit extends and connects an island or mainland to another island it becomes a tombolo (Owens, 1982). Once connected to the two land masses, the tombolo will start to form modern beaches and potentially ancient shorelines that will create strandplains (Owens, 1982). Sometimes two tombolos will form together in the same area and a lagoon may form in between the two features (Owens, 1982). The lagoon may eventually fill in, resulting in one large tombolo like the SIT (Owens, 1982).

2.3 Paleohydrographic Research

Paleohydrographic research has been completed over the past two decades by studying beach ridges, strandplains, and coastal processes throughout the upper Great Lakes and are key to understanding how lake-levels have naturally changed over decades and several millenniums.

Due to the possible threat imposed on the SIT and PBH a research group that has reconstructed lake-levels for the past six millennium in the upper Great Lakes has been contacted by the AINL managers. A paleohydrograph is a comparison of elevation and age and is also known as a “relative lake-level curve” (Johnston et al., 2014). The benefit of paleohydrograph reconstruction is that it provides a glimpse at the past natural patterns and trends of lake-levels. By comparing past records to what is occurring in the present can help create realistic scenarios for future potential lake-levels. Research within AINL has yet to be completed by this research group but they have conducted paleohydrograph reconstructions at many sites around the upper Great Lakes and created one compilation paleohydrograph for the Lake Superior outlet during the late Holocene at Sault Ste. Marie (SSM) (Johnston et al., 2012).

Normally, paleohydrographic research is conducted at sites with large embayments that have many preserved ancient shorelines or beach ridges that are dug into and cored during fieldwork to reconstruct paleohydrographs (Johnston et al., 2014). Field research was supposed to begin in Summer 2020 on the SIT at AINL but due to the COVID-19 pandemic it has been postponed. However, this pause allows for an idea in Johnston et al. (2012), which was further developed by Heather (2021) that uses topographic elevation with a correction factor and a previously reconstructed paleohydrograph to create an inferred paleohydrograph for the area which can be applied to the SIT. The inferred SIT paleohydrograph can then be compared to the fieldwork reconstructed paleohydrograph for the SIT to see if this method is viable.

2.3.1 Water Level Important Dates

Through the studies completed by the Great Lakes paleohydrographic research group, many important water level time periods have been defined down to a resolution of decades as well as a link to when Lake Superior finally separated from Lake Michigan-Huron (Johnston et al., 2014). Lake Superior has an extensive water-level history after the melting of the Laurentide Icesheet, approximately exiting the Lake Superior basin 10,000 years ago (Johnston et al., 2014). In the late Holocene, four main lake-level phases have been defined in paleohydrographs (Johnston et al., 2014). The four different time periods are the Nipissing (2,800-4,900 before present [BP]), the Algoma (1,900-2,800 BP), the Sault (900-1,900 BP), and the Sub-Sault (present to 900 BP) (Johnston et al., 2012; Johnston et al., 2014). Out of the four time periods, the Nipissing had the highest water levels, thus creating higher-elevation beach ridges in strandplains (Johnston et al., 2014). A more recent occurrence that happened between the Sault and Sub-Sault phases was the final separation of Lake Superior from Lake Michigan-Huron that occurred at $1,060 \pm 100$ BP, which helped regulate water levels in the Superior basin (Johnston et al., 2012).

2.3.2 Paleohydrograph Reconstruction through Fieldwork

To reconstruct a paleohydrograph two main components are needed, elevation and age, which are obtained from collecting samples during fieldwork (Johnston et al., 2014). Cores are collected from all beach ridges within a strandplain and are cored using vibration coring methods. Soil pits are dug into the beach ridges to sample for age dating. Elevation is collected at the base of the foreshore contact and is often cored in between the base and top of the beach ridge (Johnston et al., 2014). The samples are kept in a dark plastic material to prevent light

exposure to the sediment since light will change the age of the grains to the present time preventing optically stimulated luminescence (OSL) dating to accurately be performed. Samples are analyzed in specialized OSL labs to determine an age of the sample and hence the beach ridge. A paleohydrograph is then reconstructed with elevation and age data (Johnston et al., 2014). The process of GIA is deduced from the elevation of beach ridges at different sites that were formed at the same time. This helps compare different beach ridge strandplains occurring in common lake basins and reconstruct lake-level elevations of beach ridges back in time or when they were deposited (Johnston et al., 2014).

2.3.3 Paleohydrograph Reconstruction Through Topography

A remote paleohydrograph reconstruction method was first mentioned in Johnston et al. (2012) and further developed by Heather (2021) and can help prepare for the postponed fieldwork on the SIT in AINL. The method developed by Heather (2021) uses topographic elevation data that is corrected using a correction factor to estimate the base of the foreshore contact while the age is gathered from a comparison to a previously studied paleohydrograph. In Johnston et al. (2012) one strandplain was studied to reconstruct a paleohydrograph from coring and soil pit data and compared this to topographic elevations. A simple and consistent correction factor was applied across the entire sequence to the topographic elevation data to estimate a subsurface that might be obtained if the ridges were cored (Johnston et al., 2012). In Heather (2021) the method was expanded on using LIDAR elevations on a previously cored strandplain and by comparing the topographic LIDAR elevation to the paleohydrograph a correction factor like the one in Johnston et al. (2012) was found. To best match the elevation of the base of the foreshore contact using the elevation of the swale height with the correction factor matched the

paleohydrograph the best (Heather, 2021). Although most sites that have not been cored do have elevation data, detailed Canadian coastline elevation data is limited, but remote topographic elevation data from LIDAR is becoming more available and has an excellent resolution.

2.4 Topographic Elevation - LIDAR

LIDAR is a remote sensing method used to produce elevation data (Brock & Purkis, 2009; Kerfoot et al., 2019). LIDAR is the most accurate and rapid remote sensing application available for elevation models and has improved throughout the years with the help of the National Aeronautics and Space Administration (Brock & Purkis, 2009). Another benefit for the use of LIDAR is that it has the capabilities to bypass the foliage of the flora to reach the ground elevations (Brock & Purkis, 2009). Bypassing the foliage allows for a more accurate determination of the elevation since it normally skews the data but the ability of LIDAR to retrieve ground points is dependent on the density of the foliage (Brock & Purkis, 2009).

The method is completed by an aircraft that flies over the desired area with a compact system onboard that projects lasers to the ground and monitors how quickly they return, where the faster the lasers return, the higher the elevation is in that area (Brock & Purkis, 2009; Kerfoot et al., 2019). For coastal areas topo-bathymetry LIDAR is used since the blue-green laser emitted can be returned through the water allowing for the sediment elevation to be known, which does not occur with topographic LIDAR (Kerfoot et al., 2019). The ability to take readings through water is important for coastal areas as the elevation of the foreshore sediments can be examined during high tide or seiche in the Great Lakes.

2.5 Glacial Isostatic Adjustment

GIA occurs in the Great Lakes from the alleviation of the mass of the Laurentide Icesheet from the land after it began and continued to retreat, even up to today. GIA does not affect all areas equally since some ground surfaces experience a relative increase in elevation or a decrease in elevation over time. The amount of vertical elevation adjustments caused by this process can be determined through different methods including historic water-level gauge records or ancient shorelines used to reconstruct paleohydrographs in the Great Lakes.

2.5.1 Calculating GIA Using Lake-Level Gauge Data

Estimating GIA in the Great Lakes has been done by comparing pairs of water-level gauge records in one lake basin over time which was originally presented by Mainville and Craymer (2005). All lake-level elevations around the Great Lakes can be compared because they are all relative to the International Great Lakes Datum 1985, or IGLD85 (Mainville & Craymer, 2005). Estimates of GIA from individual gauge stations were incorporated into different generations of models predicting GIA (Figure 6) (Mainville & Craymer, 2005). From the third and fourth generation GIA models created, AINL is estimated to be decreasing approximately zero to three centimeters per century relative to the outlet for Lake Michigan-Huron (Mainville & Craymer, 2005).

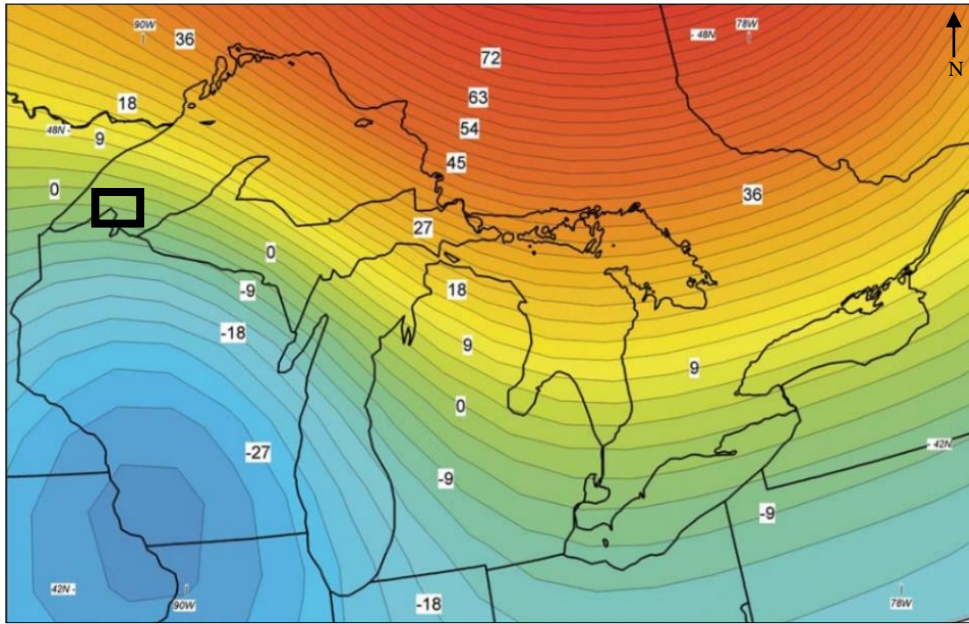


Figure 6 Third generation model created from historic water-level data. Above is an example of the model created in Mainville and Craymer (2005) where rates of GIA are represented in contours with an interval of 3cm/century. Adapted from (Mainville & Craymer, 2005).

2.5.2 Calculating GIA Using Paleohydrographs

GIA can also be calculated from data in a paleohydrograph by completing a mathematical calculation of a least squares fitted line on the paleohydrograph, accounting for the zero intercept (Johnston et al., 2014). There are two different methods that can be used to determine the least squared line, one using all beach ridge data and the other selecting certain beach ridges within a strandplain (Johnston et al., 2014). The first method that was developed by Baedke and Thompson (2000) and has the y-intercept of the line set to the current water level height of the basin outlet. This method uses the equation:

$$\log(\text{Alt}) = ax + b$$

such that “Alt” is the elevation of the beach ridge, “x” is the age of the beach ridge, and “b” is the elevation of the basin outlet based on the IGLD85 (Baedke & Thompson, 2000). From the above equation the variable “a” would be calculated and represents the GIA (Baedke &

Thompson, 2000). This is calculated for all beach ridges in one strandplain (Baedke & Thompson, 2000). The second method of calculating GIA using paleohydrographic data is done by selecting a few beach ridges within a strandplain that span through different lake-level phases such as the Sault and Nipissing phases with the line projected at the age of zero giving the approximate outlet lake-level (Johnston et al., 2012; Johnston et al., 2014). A close fit amongst the intervals is desired and is completed by repeating the procedure until data from different strandplains in one lake basin match up in the same respective time intervals (Johnston et al., 2012; Johnston et al., 2014).

2.6 Summary

The unique environment of the PBH due to its isolated location on the SIT has caused it to become endangered from the rising lake-levels in Lake Superior. Since the PBH contains endangered and threatened species, there is a concern present by the AINL managers who are mandated to protect and preserve the area (National Park Service, 2011). To better understand how to protect the PBH from rising lake-levels, the processes and features of the SIT needs to be understood prior to any research being completed on them. It can be concluded that the SIT is a previous spit that has now connected two islands and is composed of beaches and two strandplains. Understanding how the SIT possibly formed will provide more insight on how it may change. Over the past few decades strandplains have been studied by a research group to learn how lake-levels have changed around the upper Great Lakes. Though the research group that reconstructs paleohydrographs usually studies embayments for their strandplain preservation and have not studied at AINL before, the same methods can still be used to produce a paleohydrograph for the SIT. Since the research has been postponed, there is a chance to test the methods mentioned in Johnston et al. (2012) and further developed by Heather (2021). The

method allows for remote reconstruction of a paleohydrograph by using topographic elevation, a correction factor for the elevation and a previously studied paleohydrograph for age (Heather, 2021; Johnston et al., 2012). The use of topographic elevation to reconstruct a paleohydrograph is experimental and has not yet been determined accurate since topographic elevation is the only exact measurement in the method. Currently the only accurate method to reconstruct a paleohydrograph is through fieldwork and lab testing. For this undergraduate thesis, LIDAR will be used to gather topographic elevation data. The correction factor found in Heather (2021) will be used to adjust elevations, along with previously reconstructed paleohydrographs adjusted for GIA to infer ages, to reconstruct an inferred paleohydrograph for SIT.

Overall, by paleohydrograph reconstruction, it is possible to make a prediction on the fate of the SIT and the PBH caused by the rising lake-levels in Lake Superior. Though the remote reconstruction method is experimental it will provide the research group a prediction on ages of the SIT beach ridges and potentially help better predict where to core when fieldwork occurs.

3.0 Goals and Objectives

The main goal of this undergraduate thesis is to determine the potential fate of the SIT and the PBH. This can be done by reconstructing a paleohydrograph with topographic elevations retrieved from LIDAR data and ages inferred from previously studied strandplains around Lake Superior. Past lake-levels determined through the inferred paleohydrograph in this undergraduate thesis will help guide field work that has currently been postponed. By the end of this undergraduate thesis an age and elevation will be determined for each ancient shoreline and beach ridge that makes up the SIT.

4.0 Experimental Design and Methods

The method used in this thesis incorporates the collection of data in the form of LIDAR and shapefiles to produce maps of the study site as well as determine the extent of the SIT. The extent of the SIT and its strandplains is then used to retrieve elevation data to produce graphs to determine an inferred SIT paleohydrograph pattern. The inferred paleohydrograph pattern developed is then compared to another previously reconstructed paleohydrograph to determine an approximate age range of the ridges.

4.1 Collecting Data

The LIDAR data used in the analysis was obtained from Digital Coast on the NOAA website (<https://coast.noaa.gov/digitalcoast/data>). When deciding which dataset to download the decision was made by the year the data was collected and the data available. “2016 3DEP Lidar: Bayfield County, WI” by the USGS was chosen for this thesis as it was the most current source that had LIDAR points available with coverage of the SIT. When downloading the data, the use of meters was chosen for the horizontal and vertical units and the output product was chosen to be points with the output format set to LAS, the file type used for LIDAR points and all other parameters were left as the default.

Topographic map elements were also obtained from The National Map (TNM) by the USGS (<https://apps.nationalmap.gov/downloader/>). Once in the TNM Downloader version 2.0, the area of the SIT was drawn around with the extent tool and then “Topo Map Data and Topo Stylesheet” was selected along with “Shapefile” prior to clicking “Search Products”. When the results are shown the map entitled “USGS Topo Map Vector Data (Vector) 43276 Stockton Island, Wisconsin 20190325 for 7.5 x 7.5 minute Shapefile” that shows a topographic map of

Stockton Island and Presque Isle was downloaded by selecting “Download ZIP”. The topographic data was published on March 25, 2019 and is more recent than the LIDAR data.

4.2 Creating the Digital Elevation Model

Once the LIDAR and topographic map data was obtained, ArcGIS Pro version 2.6 (ESRI, 2020) was used to create a digital elevation model (DEM) and produce maps of the SIT. The first step to create the DEM was adding the LAS files to the project file and then cutting out points using the “Extract LAS” 3D analyst tool to better focus on the study site. Using the “Extract LAS” tool is done by selecting the LAS file that needs points removed, selecting and naming a destination for the new LAS file, drawing a shape around the area that is needed and then running the tool to produce the newly formed data file (M. Weiland, Personal Communication, January 26, 2021). The use of the “Extract LAS” tool was used on the LAS files to help focus on the SIT extending slightly past the extent of the SIT as defined in Figure 7. By focusing the data more on the area of SIT, the higher elevations on Stockton Island and Presque Isle were not factored into the DEM gradient and more of the colour gradient could be focused on the SIT, making the variations in the strandplains easier to see. In Figure 7 the most northern and southern extent of SIT was determined by the elevation gradient change on the DEM between Stockton Island in the north and Presque Isle in the south. The most northern extent was determined based on the Stockton Island cliff bordering the East strandplain producing a boundary between the red-yellow gradient. The lower northern extent was determined by the Stockton Island cliff bordering the West strandplain and produced a boundary between the yellow-green gradient. The southern extent of SIT was found the same way as the northern extent but the change from SIT to Presque Isle was more consistent so only one boundary was defined. The extent of the SIT strandplains were determined from the DEM

produced as the furthest visible landward ridge seen on the DEM was chosen as the extent then the extent compared to satellite imagery from Google Earth to help differentiate the strandplains from the bog.

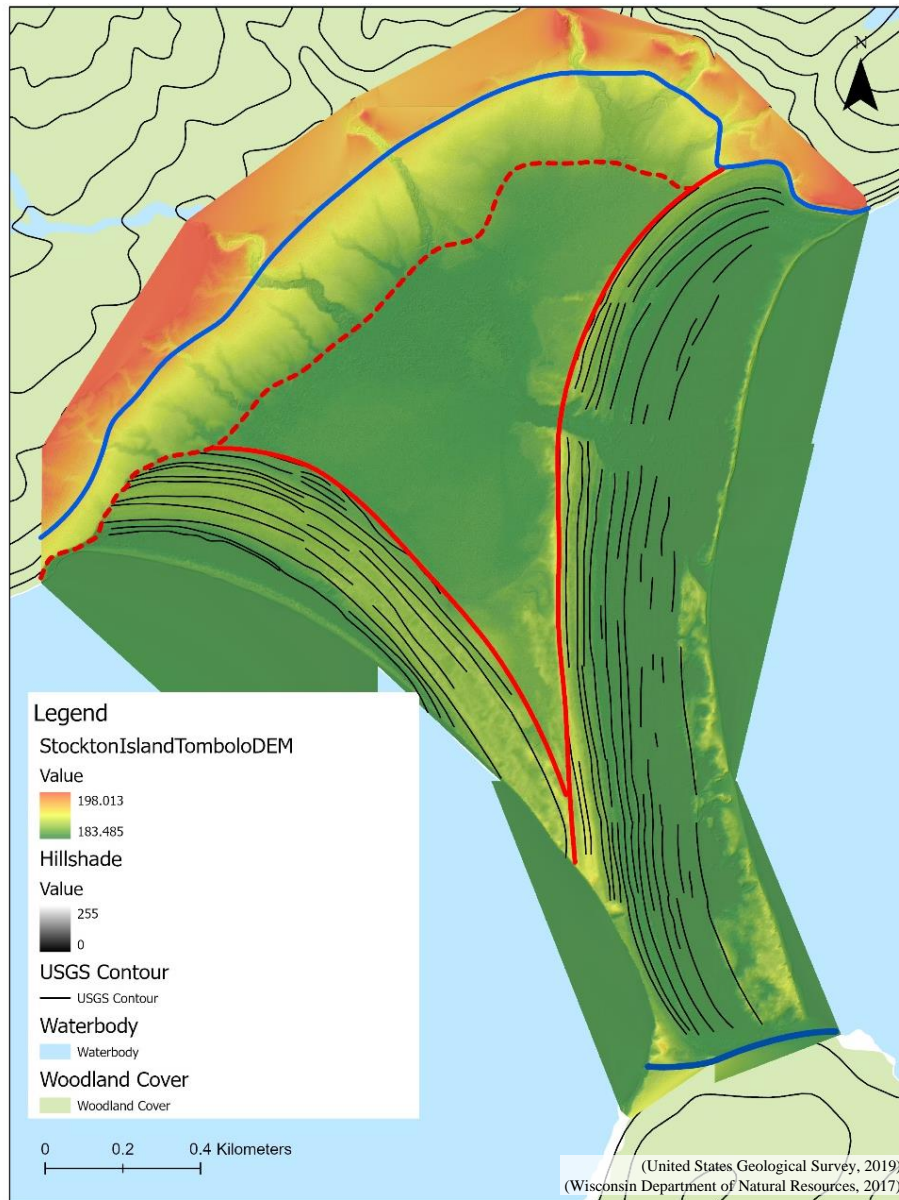


Figure 7 Extent of the SIT and location of ridges. Blue lines represent the most northern and southern extent of the SIT while the red dashed line represent the lower possible northern extent. The solid redlines represent the landward extent of the ridge and swale area or strandplain, one for the East and West strandplains.

Once all the LAS files are to the extent of the SIT, they were combined to form one LAS dataset (LASd) by using the “Create LAS Dataset” data management tool in ArcGIS Pro. Use of the “Create LAS Dataset” tool is done by selecting the LAS files that cover the extent of SIT which need to be combined and choosing an output location and name of the new LASd file (O’Neil-Dunne, J., 2019). By combining the LAS files together, it allows for the LAS files to all have the same elevation gradient with a corresponding maximum and minimum, so the colour gradient aligns to the same elevations for all files (O’Neil-Dunne, J., 2019). Then the “Make LAS Dataset Layer” data management tool was used to create a dataset where only the ground points were used allowing for a bare earth model DEM to be created (O’Neil-Dunne, J., 2019). When using the tool, the LASd layer that was formed in the previous step was selected for the input data, an output data file name was created, ground points or selection “2” was selected, and finally all returns was selected prior to running the tool to produce the dataset (O’Neil-Dunne, J., 2019). The statistics for the LASd file are then calculated by selecting the LASd file, choosing the data tab, selecting statistics then calculate statistics (O’Neil-Dunne, J., 2019). Calculating the statistics of the LASd file is important so the average spacing between the LIDAR data points is known for when the DEM raster is made (O’Neil-Dunne, J., 2019).

After the LASd layer was formed, the conversion tool “LAS Dataset to Raster” was used to take the layer created and produce it as a raster image so the elevation could be retrieved (O’Neil-Dunne, J., 2019). Once the tool was opened, the previously created LASd layer was used as the input with an output raster name created and the various fields were determined (Table 1). The value field was selected as “elevation”, interpolation type fields selected as “triangulation”, “natural neighbor”, and “no thinning”. The output data type was selected as “floating point”, sample type selected as “cell size”. The sampling value was inputted as “0.6”

based off an average taken from the calculation of the LASD file as described above and a Z factor of 1 and then running the tool to produce the DEM raster (O’Neil-Dunne, J., 2019). To be able to better see the DEM heights a hill shade was created by selecting the DEM raster and under “raster functions” within the “Analysis” tab and selecting hill shade and running the program with the default properties (O’Neil-Dunne, J., 2019). The hill shade was then placed under the DEM raster and the DEM raster was made transparent until the visually optimal balance was found (O’Neil-Dunne, J., 2019). The hill shade underneath the transparent DEM raster allows for a better visualization of the elevation from a two-dimensional image.

Table 1 Selections made to create the DEM through the “LAS Dataset to Raster” tool.

Field	Selection
Value Field	Elevation
Interpolation type	Triangulation
	Natural Neighbor
	No Thinning
Output Data Point	Floating Point
Sampling Type	Cell Size
Sampling Value	0.6
Z Factor	1

4.3 Deriving Data from Transects

To first create the transects that are perpendicular to the modern coast of SIT, two representative lines of the modern coast must be drawn. Firstly, the catalog pane was opened in ArcGIS Pro to access the folders and find the geodatabase for the project (Joyce, K., 2019b). The geodatabase is then right clicked, selecting new and then selecting feature class to open the create new feature class window (Joyce, K., 2019b). The new feature class was then named, and the class type was selected as line and is added to the map view (Joyce, K., 2019b). To create the lines along the coast, the edit tab is opened and create is chosen to be able to form the lines (Joyce, K., 2019a).

Once the lines representing the modern coast were created, the line for the West strandplain's modern coast was selected and the transects were made by using the data management tool "Generate Transects Along Lines" (M. Weiland, Personal Communication, February 3, 2021). The data management tool creates perpendicular transects along the selected line and for the purpose of this thesis the transects were spaced 100 meters apart and were 1000 meters in length. The transect length was chosen based on the length that covered all the ridges within the strandplain since if the transect was too short it would not be representative of the strandplain. The spacing between the transects along the strandplain was chosen because the transects should cover most of the strandplain to be certain all ridges are represented since some are discontinuous. Once the transects were created, the "Generate Points Along Line" tool was used to create points every 0.5 meters along the transect so there are specific points for the elevation data. By generating points, it allowed for the "Add Surface Information" 3D analyst tool to be used to add the elevation of each point to the attributes table by selecting the transect points as the set of points and the DEM raster as the source of elevation data. Once completed, the attributes table of the points generated along the transect contains elevation data as well. The process of creating transects and adding data to them was then repeated for the East strandplain. The attributes table for both the East and West strandplain transect points were exported to Excel files using the "Table to Excel" conversion tool to allow for the data to be combined and manipulated into tables and graphs.

4.4 Excel Datasets and Graphs

Using Excel 2016, the data from the attributes table were used to create graphs of topographic elevation and distance along the transect. One transect from both the East and West strandplain were chosen to best represent of their respective strandplain. To create the graphs to

compare the transect elevation, the location of the point along the transect had to be determined. This was completed by taking the point number and multiplying it by 0.5 meters since there were 2,000 points along the 1,000 meter long transect. If the point number was greater than 2,000 the point numbers would have the previous number that is evenly divisible by 2,000 used. For instance, if the point number was 12,000, the formula “ $= (12,000-10,000)*0.5$ ” was used to find the distance along the transect.

Once the distance was determined, the graphs were made as scatterplots with straight lines between data points to better see the peaks of the ridges. From there one representative transect was chosen from the West and East strandplains based on the common pattern between transects and the number of visible ridges within the DEM. The topographic elevation data then needed to be adjusted to estimate the subsurface elevations, a proxy of past lake level elevations, for each ridge (Johnston et al., 2014). Johnston et al. (2012) suggested subtracting 1.5 meters from field measured topographic elevations in a strandplain at SSM while Heather (2021) further refined and developed the method from LIDAR data. Heather (2021) suggests using individual distances from ridge crests and the elevation of their respective swales to create a topographically inferred paleohydrograph (using distance instead of age). Then by taking the elevation of the swales and subtracting 1.49 meters would be a good representation of past lake level that somewhat relates to the base of the foreshore contact that is obtained from cores with fieldwork. Once the subsurface contact was found for representative transects for the East and West strandplains, the two transects were combined to create a subsurface inferred paleohydrograph. This subsurface inferred paleohydrograph (with distance instead of age) would be a relatively good estimate of past lake level if fieldwork has not been completed and LIDAR data is available.

However, for a paleohydrograph to be reconstructed, ages need to be assigned to each ridge from the strandplain data. To estimate the ages of the ridges at SIT, cross-strandplain geomorphic trends and patterns have been accounted for (Johnston et al., 2007) and rates of GIA were applied to be able to compare paleohydrographs with assigned ages in other strandplains to the SIT inferred paleohydrograph pattern (Johnston et al., 2012 and 2014). To determine the ages of the ridges the SSM outlet paleohydrograph (Johnston et al., 2012) was chosen and adjusted with different rates of GIA. Once the SSM outlet paleohydrograph was adjusted the SIT inferred paleohydrograph pattern was aligned to the curve based on overall trend and elevation and approximated ages were found.

5.0 Results and Discussion

5.1 Raw LIDAR Data

When the LIDAR data was downloaded from Digital Coast it came as six different LAS files where only four were related to the tombolo and were used. Since the data extended past the boundaries of the SIT the “Extract LAS” tool was used so it only slightly exceeded the tombolo as seen in Figure 8. To allow all LAS files to have the same elevation gradient they were combined into a LASd file and produced the map seen in Figure 9. Then a LASd layer of all returns of ground points was produced from seen in Figure 10 which allowed for a bare earth DEM to be created. From there the DEM raster and hill shade were produced and created the final DEM that will be used to derive the elevation for the transects.

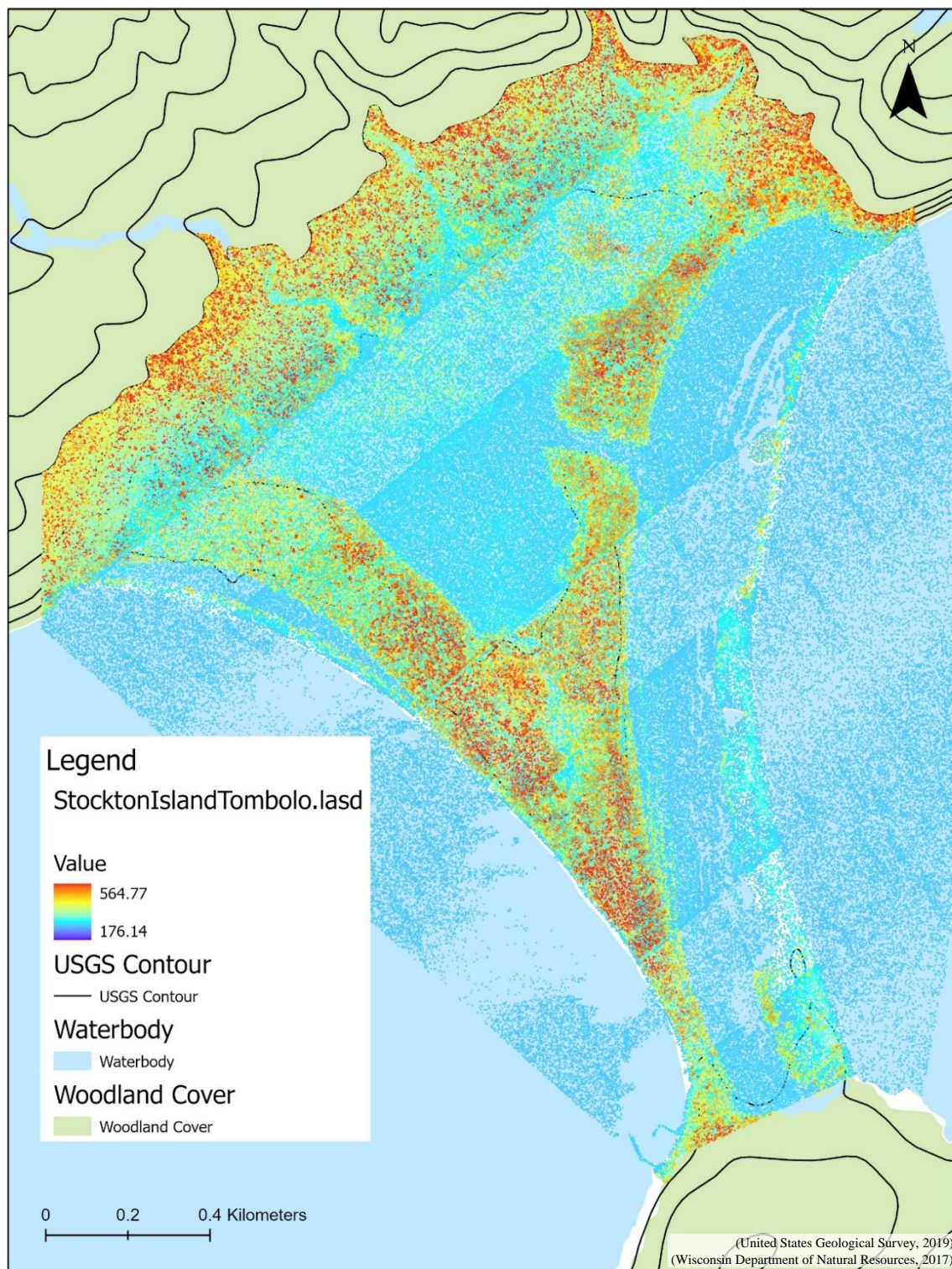


Figure 8 LIDAR dataset (LASd) created from combining the four LAS files. The LASd allowed for one elevation gradient to be used but still had the tops of trees and other features as highpoints and not ground points.

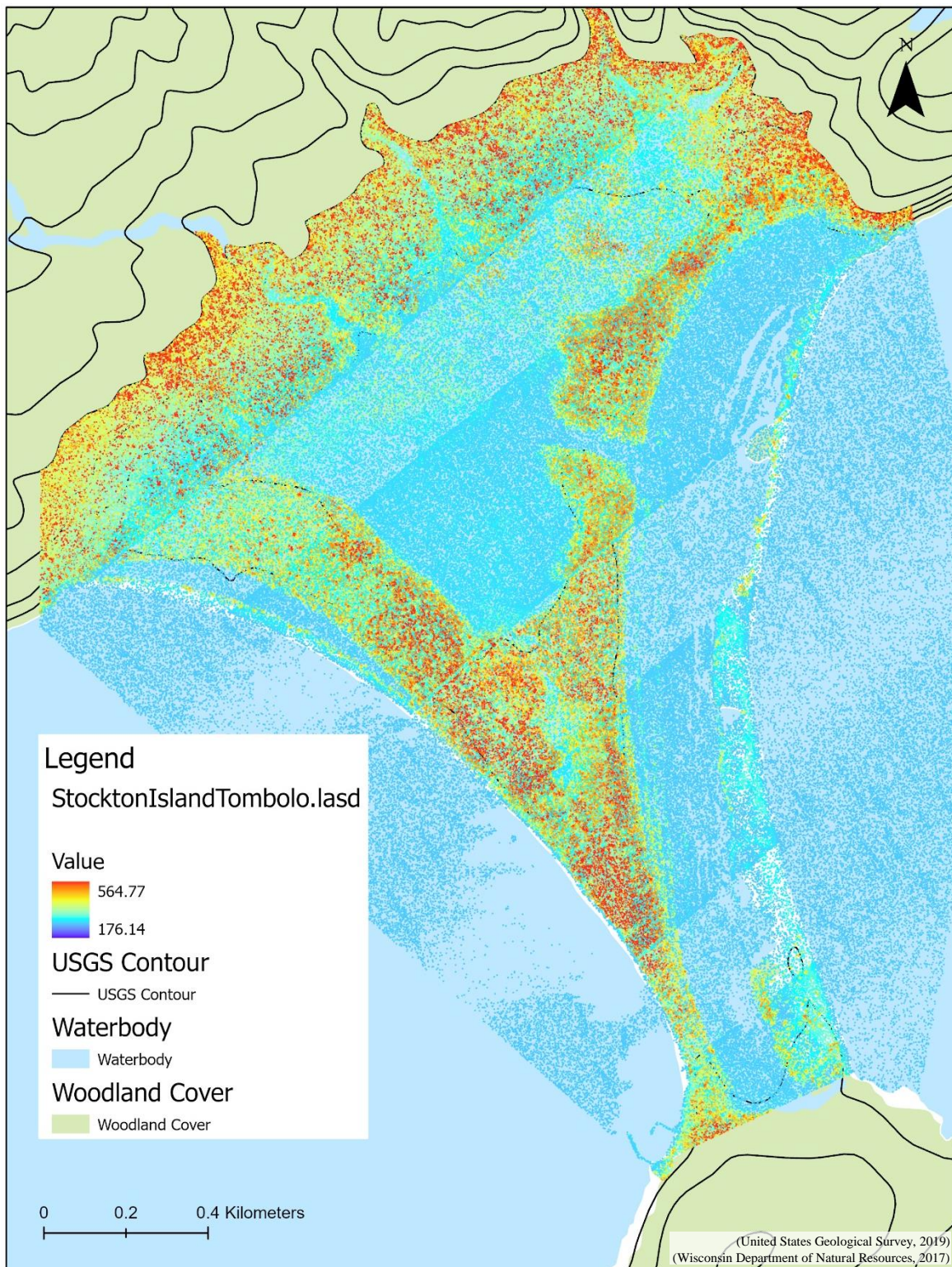


Figure 9 LIDAR dataset (LASd) created from combining the four LAS files. The LASd allowed for one elevation gradient to be used but still had the tops of trees and other features as highpoints and not ground points.

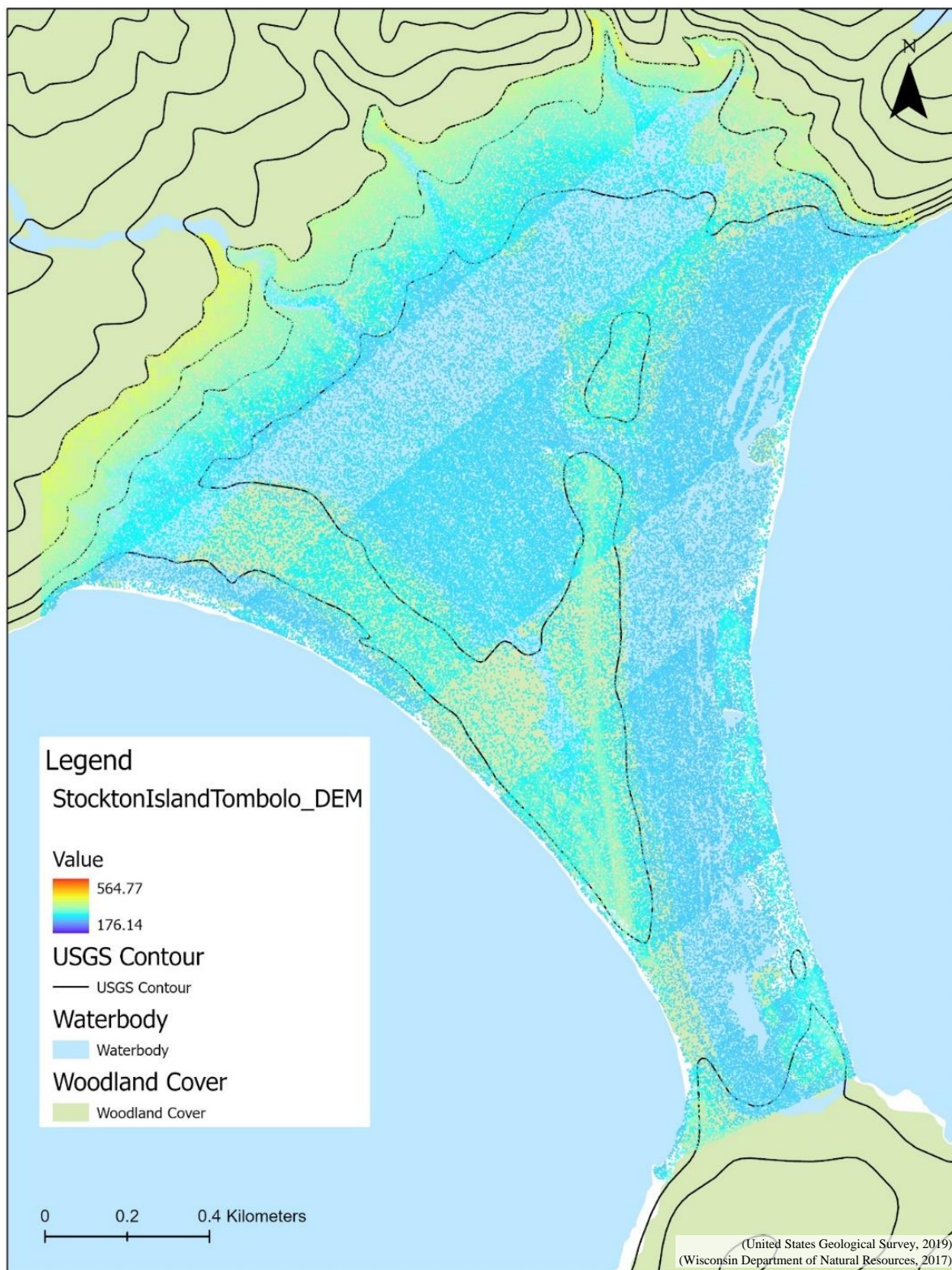


Figure 10 LIDAR dataset ground points layer. The treetops and other elevated surfaces that were not related to the ground have been removed. The highest points on the map are in the northern portion of the LIDAR points.

5.2 Digital Elevation Model

Once the DEM was created, the extent of the SIT was able to be determined through the colour gradation changes and topography of the area seen in Figure 11. The northern extent has two different possible locations. The first northern extent is shown by the solid blue line was determined by where the East strandplain meets the cliff of Stockton Island and follows the red-yellow boundary which was then extended to the other west side of the tombolo. The second northern boundary was determined by where the West strandplain meets Stockton Island at the yellow-green boundary and was followed to the other side of the SIT. The red-yellow boundary elevation ranges from 190.0 to 192.0 meters while the yellow-green boundary elevation ranges from 185.5-187.5 meters. The southern boundary was determined in a similar approach by determining the location of the increase of elevation due to Presque Isle and is represented by the southern blue line with elevation range of 186.5 to 188.0 meters. Finally, the boundaries of the West and East strandplains were determined mainly through elevation changes visible in the DEM and referencing satellite imagery from Google Earth. The visible difference between the two strandplains in the satellite imagery was seen through the vegetation changes since the strandplains tend to end where the bog begins which is seen by the pine trees that inhabit the strandplains. Though the vegetation is a good indication, there are some overlap of the trees between the strandplains and bog where blowouts and washovers have occurred on the ridges. The boundaries of the East and West strandplains can be seen by the solid red lines, which were chosen using the most landward ridge on each strandplain.

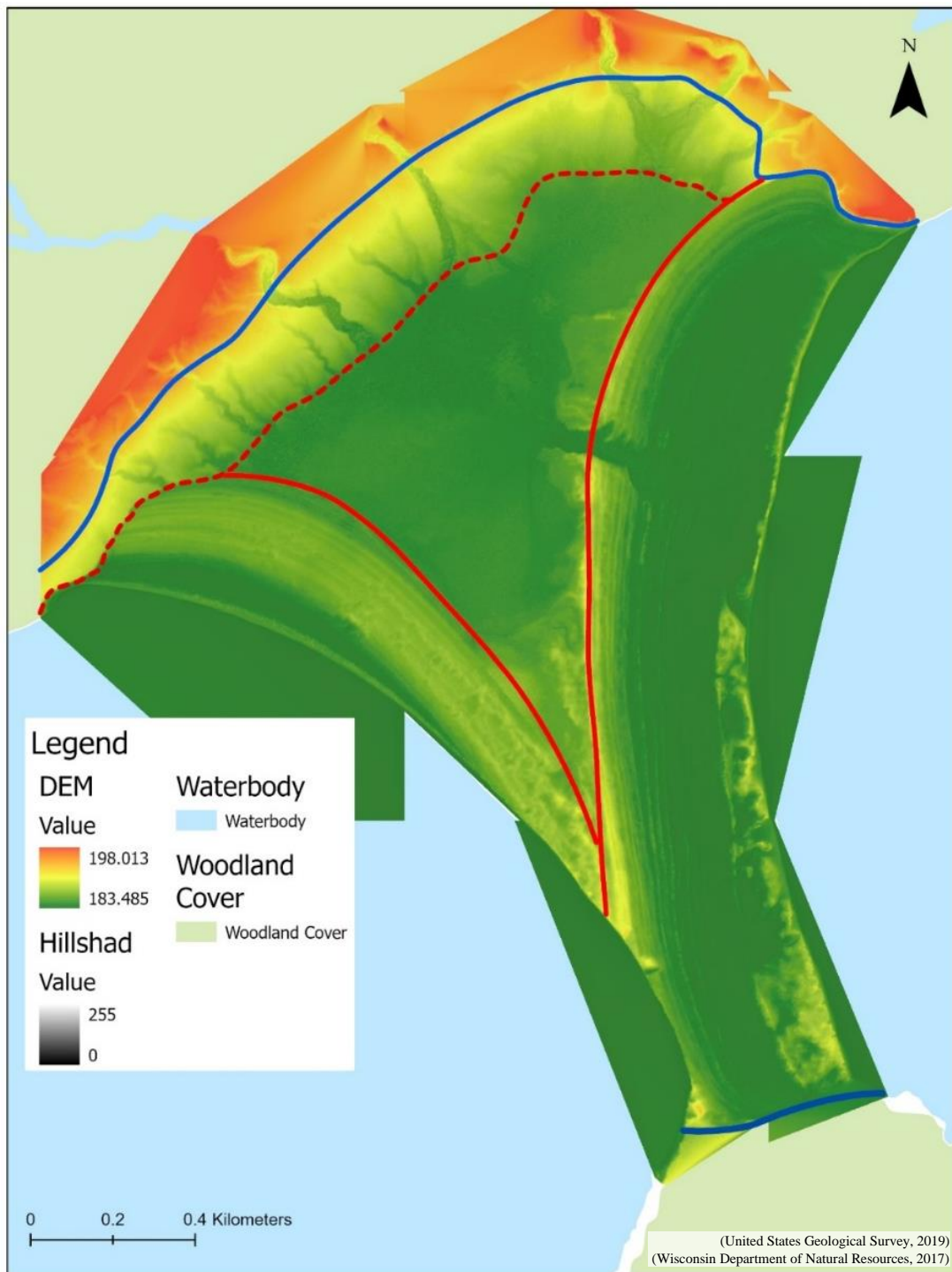


Figure 11 Extent of the Stockton Island Tombolo and its strandplains. Strandplain locations are denoted by a solid redline. The solid blue lines denote the farthest north and south boundaries of the tombolo while the dashed redline shows a possible intermediate northern boundary.

By visual observation of the final DEM all the visible ridges in each strandplain (east and west) were determined and marked on the map in Figure 12. Generally, the West strandplain ridges are formed in a northwest-southeast direction and have an arcuate shape. In the West strandplain the ridges are more continuous in the north portion of the strandplain while the southern portion of the strandplain has less ridges and they are not as continuous. Also, the ridges appear more continuous further inland than the ridges closer to the lake. In the East strandplain the ridges form more north-south in the southern half while it becomes more northeast-southwest orientation in the northern half of the strandplain and is also in the shape of an arc, but the curve is less pronounced than the West strandplain. The ridges in the East strandplain tend to be more continuous further inland than the ridges closer to the lake except for the ridge right beside the water where it is continuous except at the creek outlet. For both strandplains the maximum number of ridges occurs at the peak or turning point of the arc resulting in 13 ridges in the West strandplain and 12 ridges in the East strandplain.

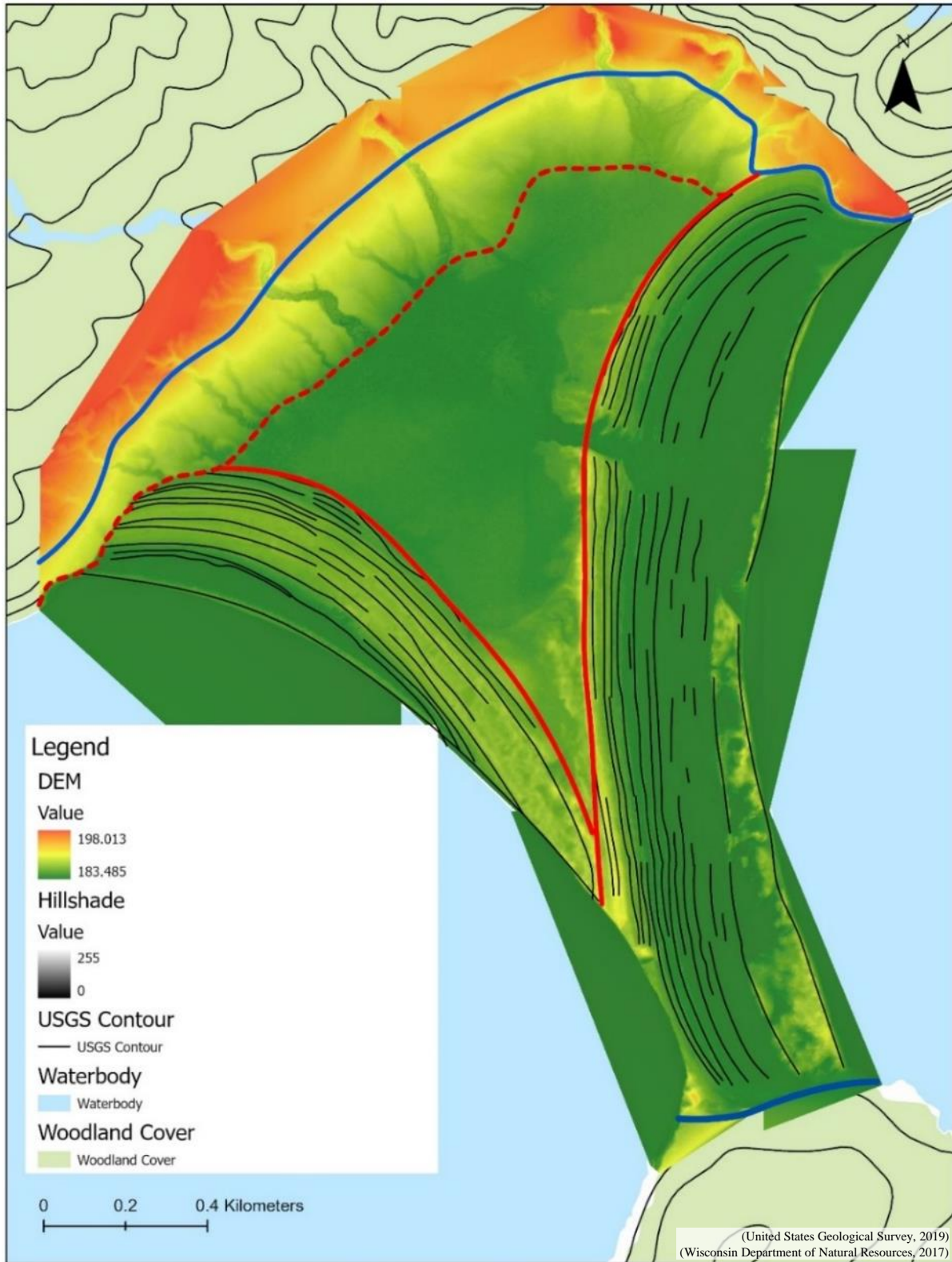


Figure 12 Location of ridges in the East and West strandplains. Locations of the visible ridges within the DEM for both the East and West strandplains.

5.3 Topographic Transects

Transects were created to find trends and patterns within the East and West strandplains and were drawn to be perpendicular to the coast of their respective strandplain. The transects then allowed for elevation data to be collected for each point along it and the points were graphed to see the trends and patterns of each transect. On the West strandplain 17 transects were created with transect zero being the northernmost transect and transect 16 being the southernmost transect. The East strandplain had a total of 24 transects where transect 0 was the northernmost transect and transect 23 was the southernmost transect.

When creating the transects, the length of 1000 meters was chosen since it would allow all the transects to cover their necessary area. For instance, transect five (6th from the north counting towards the south in Figure 13) of the East strandplain has slightly more distance to cover all ridges and swales while transect one (below transect 0 counting from the north in Figure 13) has extra distance that exceeds the strandplain. The spacing between the transects was chosen to be somewhat equally spaced between one another to avoid repetition but also obtaining enough data and detail to find common patterns in the topography representative of each strandplain. The resulting transects, Figure 13, then had points added along the transects at a spacing of 0.5 meters so elevation could be collected along the transect while not be missing ridges due to spacing of the points. The elevation data added to the points of the transect allowed for the data to be exported to a spreadsheet (Excel) and graphed.

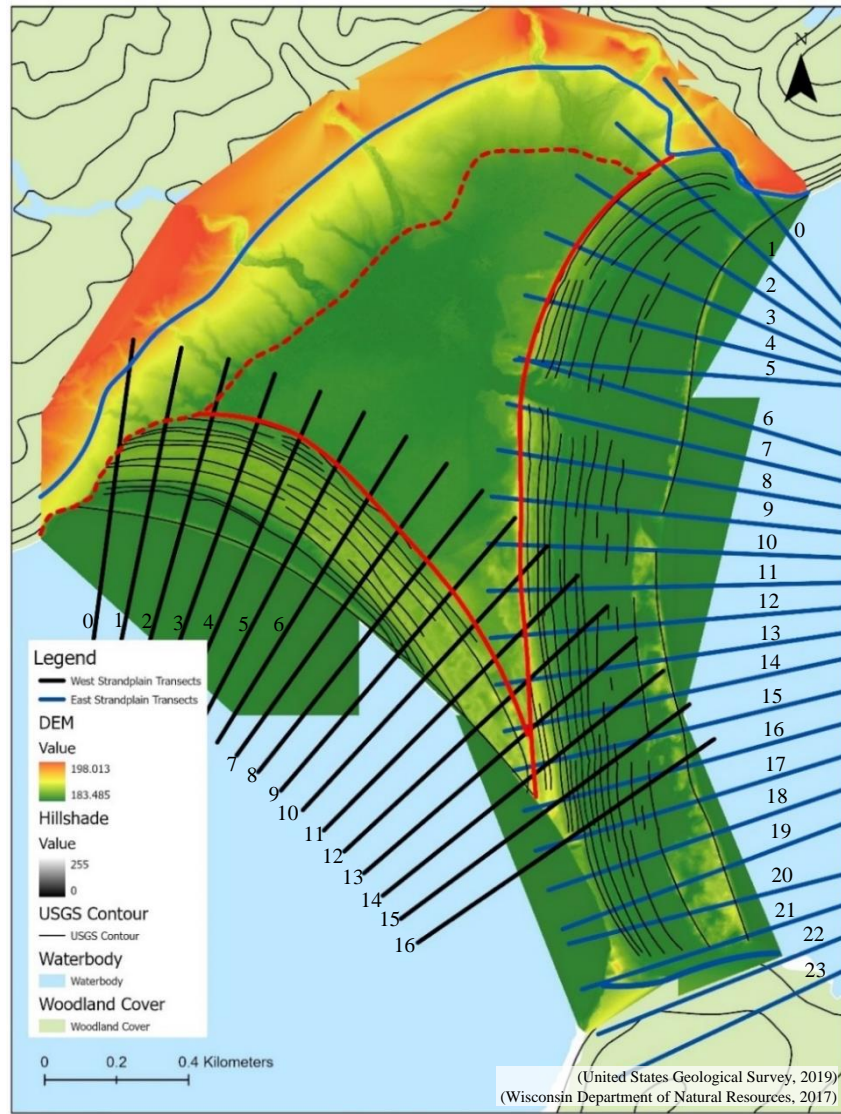


Figure 13 Locations of transects for both the East and West strandplains. The West strandplain begins with transect 0 being the northernmost transect and ending with transect 16 being the southernmost transect. The numbering convention is the same for the East strandplain with 0 being the northernmost transect and 23 being the southernmost transect.

5.4 Excel Data

The resulting graphs of the transects for the East and West strandplains can be seen in Figure 14 a-f and were used to help determine the best representative transect for each strandplain. Since transects 0 and 1 in the West strandplain as well as transects 0, 22, and 23 in the East strandplain did not cover the tombolo but rather Stockton Island and Presque Isle they

were not representative of their strandplain and were not included in the graphs. Transects 14, 15, and 16 were also removed from the West strandplain graphs as they covered data in the East strandplain which is not represent the West strandplain. Graphing the data helped to differentiate ridges and swales and determine one common pattern, representative of each strandplain. The representative transect was also determined based on the number of visible ridges through each transect.

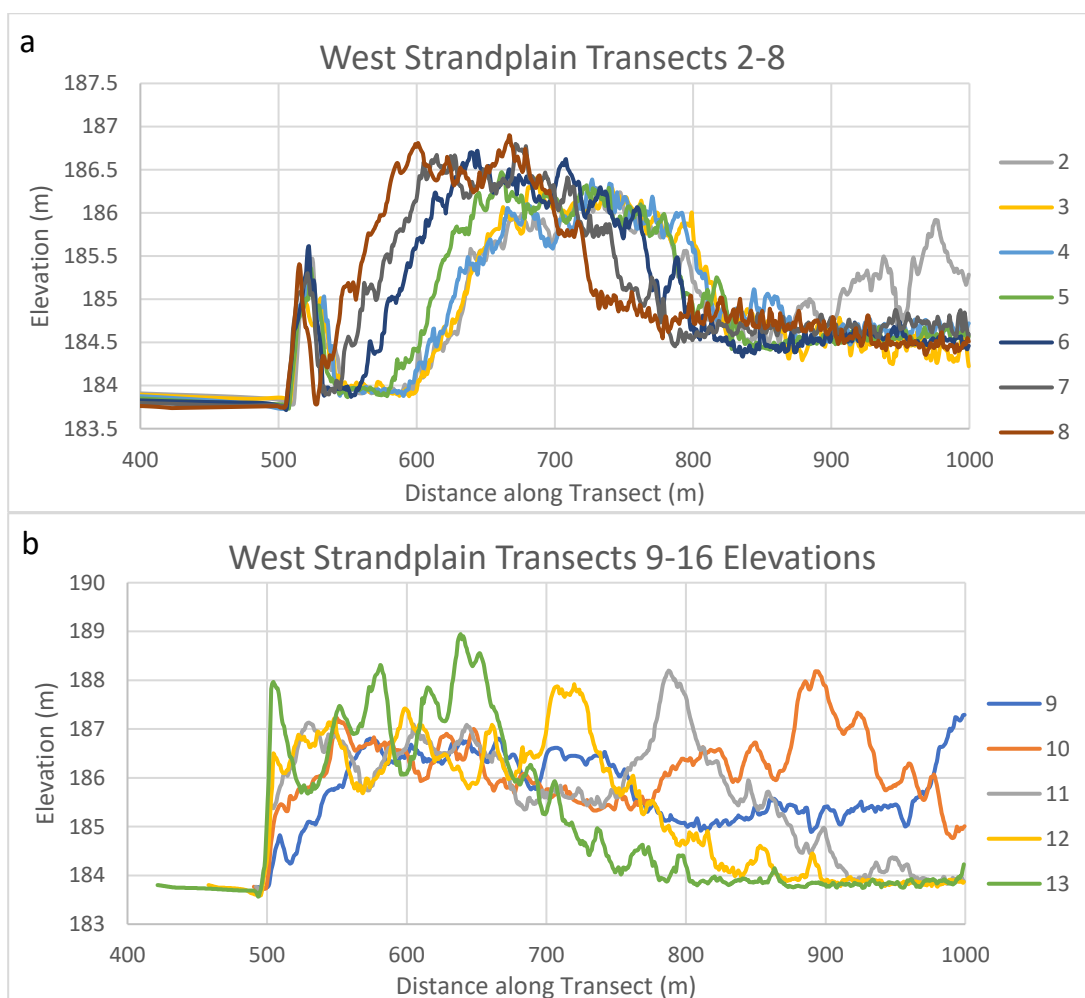


Figure 14 Topographic elevation derived from the LIDAR DEM versus distance inland of the strandplain transects. a) Topographic elevation of West strandplain transects 2-8 which follow a pattern starting at the most landward ridge of a rising, a leveling, a lowering, another leveling then one high ridge beside the lake. b) Topographic elevation of West strandplain transects 9-16 had a pattern that is not aligned together by distance as seen in *a* and the number of ridges and swales are limited.

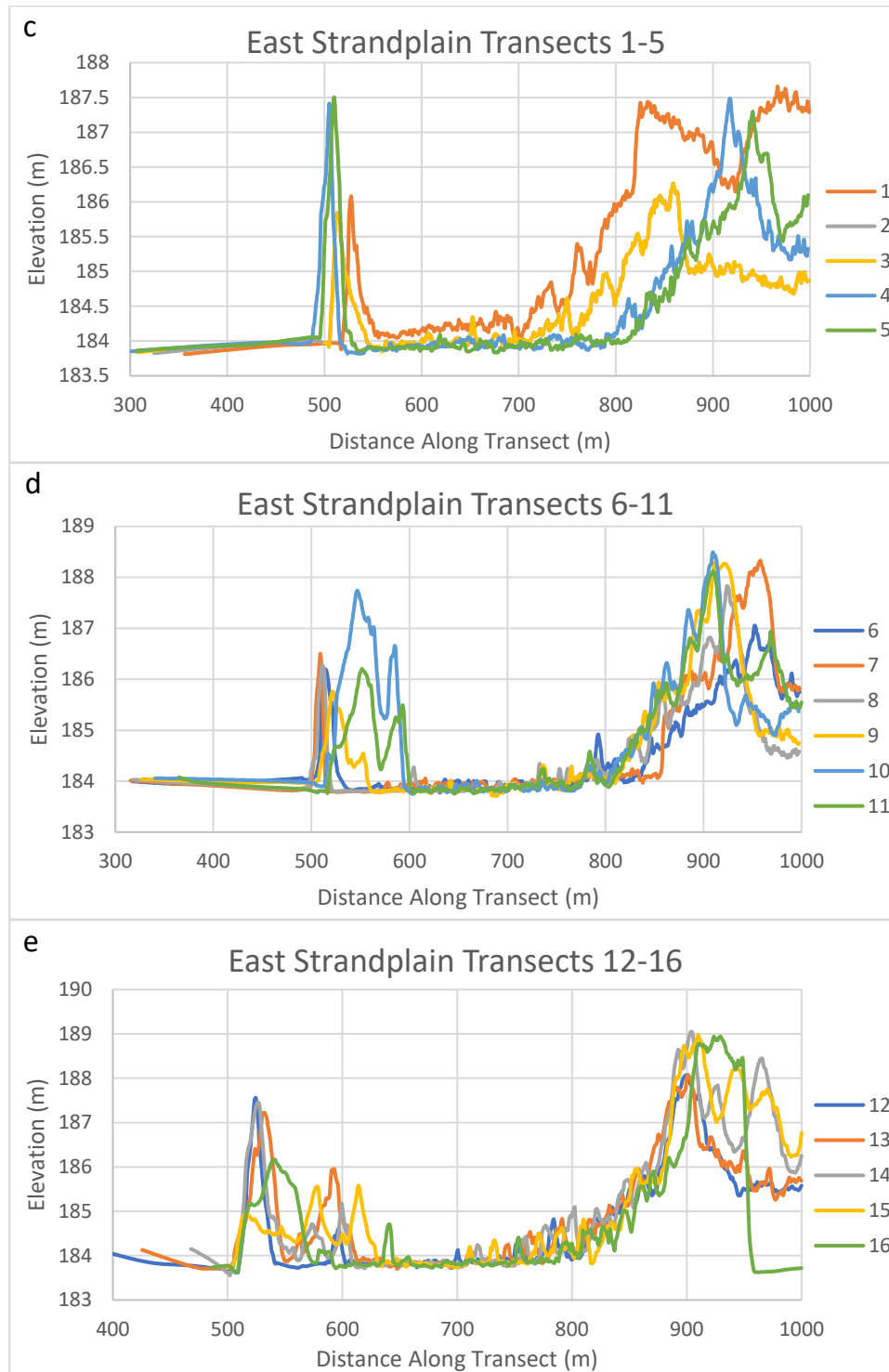


Figure 14 Topographic elevation derived from the LIDAR DEM versus distance inland of the strandplain transects. All transects in these graphs c-e follow the same pattern starting at the most landward ridge, a lowering, a leveling and then a high elevation ridge by the lake and are representative of the East strandplain. c) Elevation of transects 1-5. d) Elevation of transects 6-11. e) Elevation of transects 12-16 some of the ridges closest to the lake deviate from the common pattern.

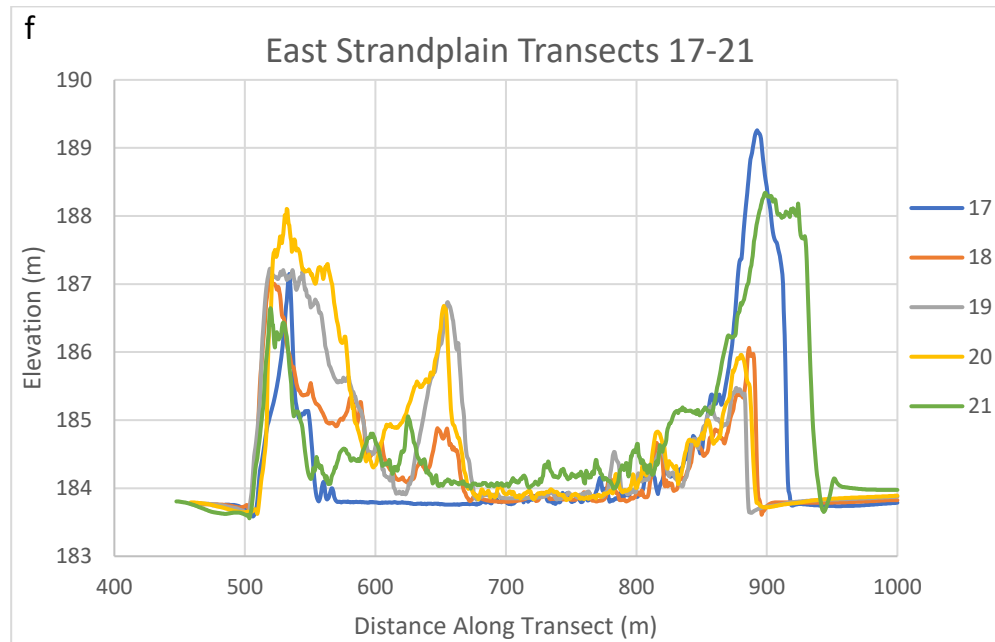


Figure 14 Topographic elevation derived from the LIDAR DEM versus distance inland of the strandplain transects. f) Transects 17-21 in the East strandplain where the pattern follows the same one seen in c-e but the ridge beside the lake is extended further inland until about 675 meters along the transect most likely due from blowouts and washovers.

In the West strandplain a common pattern that is described from the landward to lakeward ridges (east to west) can be seen with transects 2-8 but is not as clear or different in transects 9-16. For transects 2-8 in Figure 14a, starting in the most landward side of the graph (distance of 1000 m), there is a leveling representative of the bog area, that proceeds into a rise (beginning of the strandplain) that increases elevation by approximately two meters and occurs for approximately 100 meters. The rise then turns into a leveling phase that lasts for about 125 meters that is then followed by a lowering where the elevation lowers to around 184 meters in all transects. Transects 2-5 show a larger second leveling than transects 6-8 prior to reaching the most lakeward ridge of the SIT that has an elevation of 185 to 185.5 meters. For transects 9-13 a common pattern occurs starting at the most landward ridge as a leveling, a short rise, another leveling then a lowering to Lake Superior. The common pattern seen within transects 9-13 seen in Figure 14b is not as similar between the transects as it is with transects 2-8, which can be

explained by looking at the DEM. When looking at the location of transects 9-13 in the DEM, fan-shaped features potentially caused by water (washovers) and/or wind (blowouts) can be seen within the area, but also there are less visible ridges in this portion of the West strandplain than the northern half of the strandplain.

For the West strandplain the transects were chosen by the common pattern seen in transects 2-8 that does not have as many washovers and blowouts seen in the DEM and when compared, transects 3-5 were the least spread out from each other as seen in Figure 14a. The stretching of the pattern between the transects is something that occurs with embayments where ridges laterally fill the embayments forming many arcuate ridges separated by swales. The most representative location is near the peak of the arc (transects 3-5) rather than the ends of the arc because that is where the ridges are the most preserved in the strandplain and are most laterally separated (c.f. Johnston et al., 2014). To determine which transect contains the most ridges, the visible ridges in Figure 13 were counted for transects 3-5 resulting in transect 4 having the most visible ridges (13 ridges) on the DEM and being the representative transect for the West strandplain.

In the East strandplain a common pattern can be seen throughout Figure 14c-f by looking at the most landward ridge to the most lakeward ridge (west to east). Starting at the most landward point in the graph (1000 meters) there is a rise and a gradual lowering that occurs for approximately 150 meters followed by a leveling that occurs for 200-300 meters. The ridges then return to a rise and a lowering for the ridge closest to the lake but is variable how many ridges appear in the graph depending on the location across the strandplain. For instance, transects 1-8, 12 and 14 show only one single high elevation ridge with a steep rising while the other transects show a rising that is more gradual, but the transects with a gradual rise also have

a shorter previous leveling section that is about 200 meters. When looking at Figure 13, the reason why the lakeward rising is more spread out in the southern transects is due to washovers and blowouts that can be seen by their fan-shape in this section of the strandplain.

The transects were narrowed down to transects 4-17 showing a common pattern seen in Figure 14c-e for the East strandplain. To determine which transect would have the best representation visible ridges noted on the DEM in Figure 13 are counted based on if they crossed the transect. Counting the ridges on the DEM resulted in transects 8 and 16 both having the highest number of crossed ridges (12 ridges) and the other transects having less visible ridges seen on the DEM. To determine which one transect to choose as the representative of the East strandplain, the DEM in Figure 13 was referred to again to determine if the swale height has been changed due to washovers and blowouts on the edge of ridges and compared to Figure 14d-e. When referencing the DEM, it was seen that transect 16 swales contained more blowouts and washovers than the swales in transect 8 and the most lakeward ridge extends further inland in transect 16 than the single ridge in transect 8. Since transect 8 has less elevation changes related to potential blowouts and washovers, it was chosen as the one representative transect for the East strandplain. The data from the two representative transects is then used to estimate the base of the foreshore contact, a proxy for past lake level.

5.5 Selecting and Adjusting Topographic Elevation

Paleohydrographs are reconstructed using the base of the foreshore contact elevation which best represents the past lake level elevation for when each ridge formed in a strandplain (Johnston et al., 2012 and 2014). For this thesis, the DEM was created from LIDAR data which is topographic data that needs a correction factor applied to the data to estimate the ancient lake

level elevation. The potential use of a correction factor was first mentioned in Johnston et al. (2012) and then developed by Heather (2021). Heather (2021) related topographic data from LIDAR and field surveying across the SSM strandplain to core data examining basal foreshore contacts to create a topographically inferred paleohydrograph. It was found that the lowest elevation in swales was relatively good to use for estimating a paleohydrograph with a correction factor of 1.49 meters to lower the topographic elevation to the approximate base of the foreshore contact elevation in SSM ridges (Heather, 2021). Although the method worked to create the paleohydrograph from select topographic LIDAR elevations it is cautioned that this new method has only been attempted at one location (SSM strandplain) where subsurface coring data was available. And this has only been tested in ridges formed during the Nipissing phase (Heather, 2021). This method and correction factor have been cautiously chosen in this thesis to reconstruct an inferred SIT paleohydrograph without any field data. It is possible that the correction factor could be different at the SIT than the SSM strandplain in Heather (2021).

To apply the method described in Heather (2021), the estimated base of the foreshore contact from topographic LIDAR elevation data needs to be found. First the swales within the graph data must be determined. To identify the location of the swales, the ridges determined in Figure 12 were found on the graph to have a starting point. Then the elevation data was followed until the lowest point of elevation was found for either side from the peak of the ridge, where the lowest point would be the base of the swale. The distance and elevation correlating with the location was then extracted from the transect data derived from the DEM and placed into another dataset. Finding the lowest point of the swale was applied to all ridges in both the West and East representative strandplain transects.

After the distance (relative to the modern shoreline) and elevations of all the swales (relative to IGLD85) were collected, the correction factor of 1.49 meters from Heather (2021) was applied to all swale topographic elevations. After subtracting the 1.49 meters from the swale elevations, this inferred the base of the foreshore contact elevation, a proxy for ancient lake level for each ridge in a strandplain. Once all the calculations were completed, the West and East strandplain elevations were compared (Figure 15 and 16). The East and West strandplain datasets did not line up on the plot as expected (Figure 15) because the distance and number of preserved ridges and swales varied between strandplains. Both datasets were also presumed to be continuous sequences at first. Since age data was not available, distances had to be adjusted to match the East and West strandplain elevations. This then help estimate the age of ridges by aligning both datasets into one, creating a representative distance versus elevation plot for the SIT. Before they could be combined some help was needed to determine how to adjust the distances so the strandplains match each other. One common discontinuity that is found within strandplains around Lake Superior could help interpret the SIT strandplains.

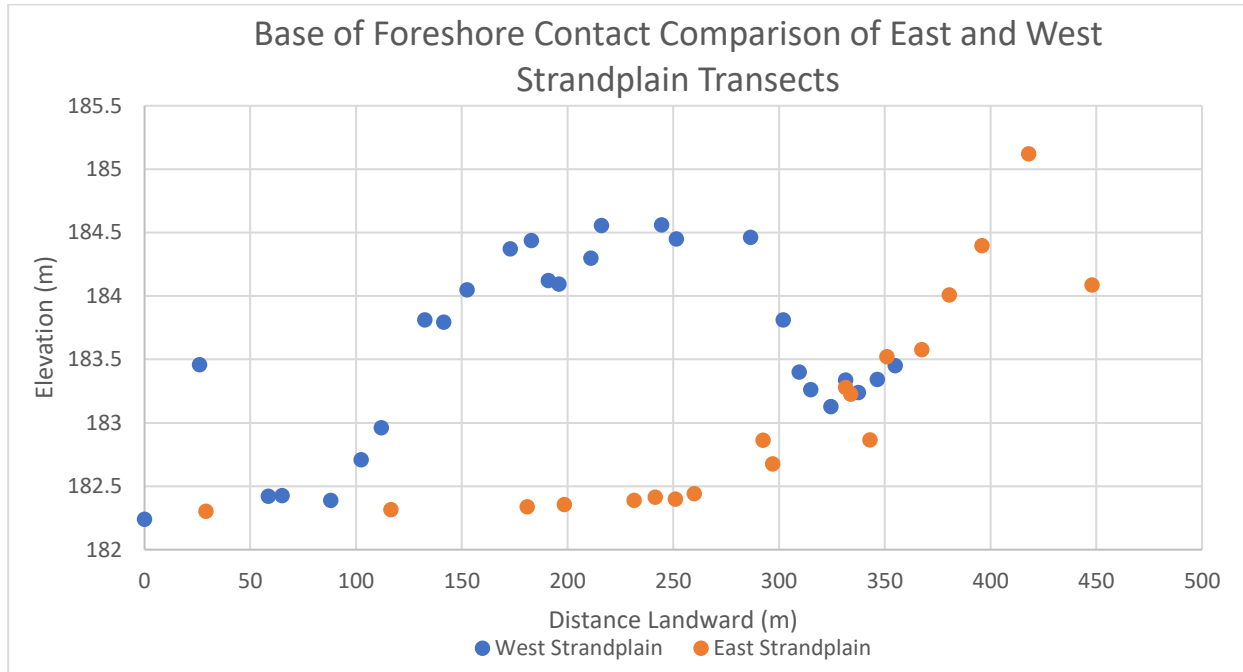


Figure 15 Comparison of the West and East strandplains with derived elevation for the base of the foreshore contact and distance landward. Starting at the most landward ridge, the West strandplain has a pattern of a rising, leveling, lowering then a final leveling phase with a potential outlier at 26 meters landward. The East strandplain has a pattern starting at the most landward ridge of a lowering and then a leveling.

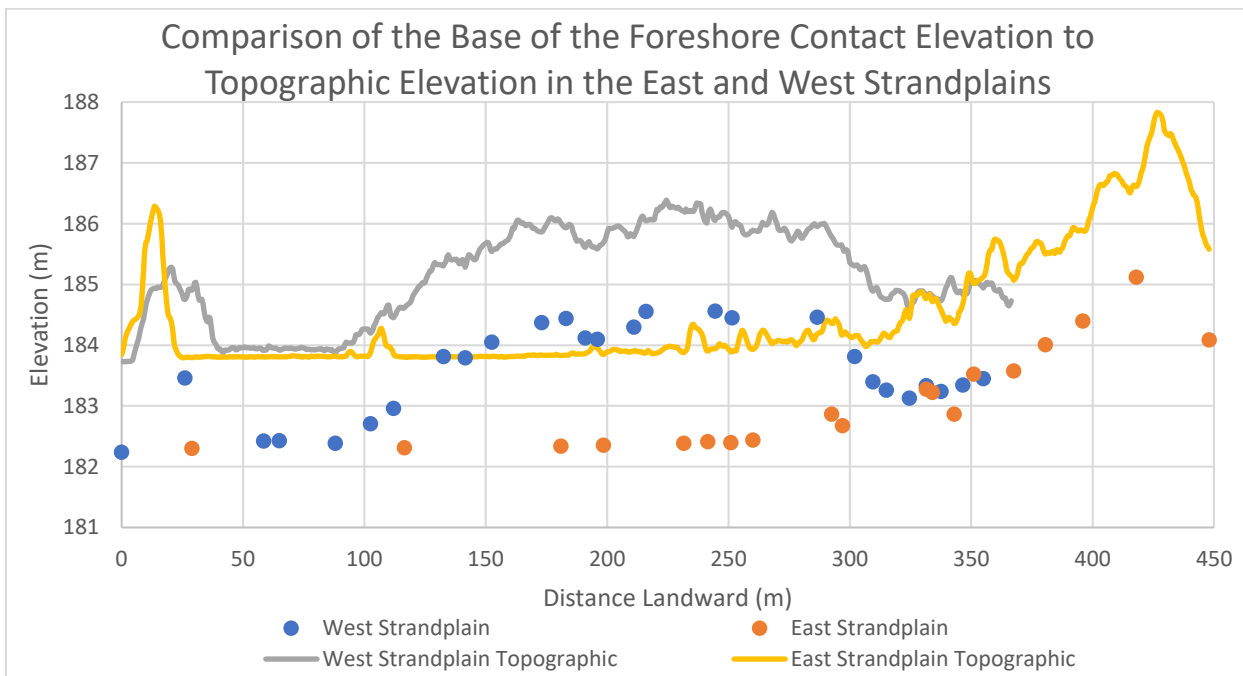


Figure 16 Comparison of the elevations for the base of the foreshore contact and the topographic LIDAR elevations. The overall pattern between the two types of elevations is the same for their respective strandplain but have different elevations due to the correction factor.

5.6 Common Discontinuity in the Lake Superior Strandplains

In the strandplains that surround Lake Superior, a common discontinuity is found and often breaks the strandplain into two areas, lakeward and landward ridges and is often determined by geomorphic and sedimentological characteristics (Johnston et al., 2007). Since this discontinuity is common across the Lake Superior strandplains then it is likely occurring at the SIT as well and could explain why the East and West strandplain elevation versus distance data does not align.

If a discontinuity exists in the SIT, then the common geomorphic characteristics can be used to determine the lakeward and landward ridges. The sedimentological characteristics cannot be used to determine the discontinuity as data from cores is required and is not currently available. To divide the strandplains into lakeward and landward segments the geomorphic characteristics of cross-strandplain trend in topography, drainage, vegetation density, ridge characteristics and swale characteristics seen in Table 2 were used. To determine the characteristics Figure 14 and Google Earth satellite imaging were used.

Table 2 Criteria to determine landward and lakeward sections of the East and West strandplain based on geomorphic characteristics. Criteria for each case was determined from Johnston et al. (2007), with the data derived from Figure 14 graphs and satellite imaging from Google Earth.

Feature	West Strandplain		East Strandplain	
	Lakeward	Landward	Lakeward	Landward
Cross-strandplain trend in topography (landward to lakeward)	Stable	Rises, stable, then lowers	Stable	Lowers
Drainage Characteristics	No drainage present		Creek bends and increases in width; sloughs	
Estimated Vegetation Density	Lower	Higher	Lower	Higher
Ridge and Swale				
a) Lateral continuity	Discontinuous to Continuous	More Continuous	Discontinuous to Continuous	More Continuous
b) Orientation	NW-SSE	NNW-SSE	NNE-SSW	NNE-SSW
Swale Characteristics				
a) Standing Water	No	No	Yes	No
b) Peat present	No	Unsure	Yes	Unsure

The main factors for determining the landward and lakeward sections are continuity of ridges, density of vegetation and cross-strandplain trends within the topography since the lakeward and landward ridges have different characteristics from each other in these factors. By using the three factors determined from Table 2 measurements of the lakeward and landward sections could be determined through Google Earth satellite imaging for the SIT. To help determine the location of the discontinuity, the distance of the lakeward and landward portions of the strandplains were found since the lakeward ridges are younger than the landward ridges. The lakeward portion of the West strandplain is approximately 90 meters wide with three ridges visible in the DEM (Figure 12) while the East strandplain is approximately 225 meters wide with six ridges visible in the DEM. This could mean that the East strandplain likely preserved more younger ridges than the West strandplain. For the landward section of ridges, the East strandplain was approximately 220 meters wide with six ridges visible in the DEM while the

West strandplain ridges were approximately 260 meters wide with ten ridges visible in the DEM. Since there were more ridges in the lakeward section of the East strandplain than the West strandplain and there are more landward ridges in the West strandplain than the East strandplain it can be inferred that the East strandplain preserved more lakeward ridges while the West strandplain preserved more landward ridges.

Common trends and patterns that often occur within strandplains around the upper Great Lakes can also be used to help decide if a discontinuity exists. The common pattern that strandplains form can be seen in Figure 17 where at a rate of GIA of zero centimeters per century (cm/century), the pattern starting at the most lakeward point will see a leveling that goes into a rise, another leveling and then a lowering before the pattern is repeated (Johnston et al., 2014). The location of the rate of GIA of zero aligns with the outlet of the lake and in the case of Lake Superior areas that are southwest of the zero isobase have negative GIA while areas that are northeast of the isobase have a positive GIA. If the rate of GIA is not at zero but is positive and adding elevation to the area an overall lowering trend would occur and is seen by the top three curves in Figure 17 (Johnston et al., 2014). The lower three curves in Figure 17 shows the overall lake level trend that is rising because the rate of GIA in this area is lower than zero causing the area to be lower than the center of the waterplane at the outlet (Johnston et al., 2014).

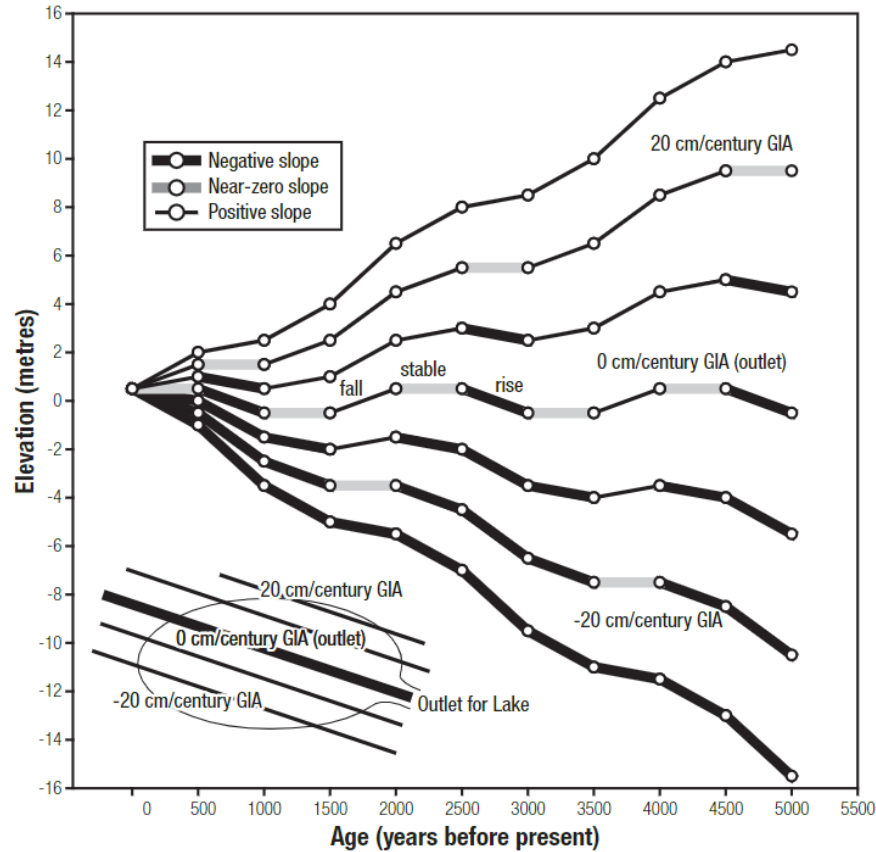


Figure 17 Change of paleohydrograph slope based on the rate of glacial isostatic adjustment. When the rate of GIA is at zero, which is the same rate as the active outlet, the baseline pattern of a rising, leveling, lowering, and then a leveling occurs. When the rate of GIA is a positive number, meaning the area is generally rising faster than the outlet, the pattern adjusts to show an overall lowering effect. When the overall area is rebounding slower than the outlet, the rate of GIA is negative, and the overall trend appears to be rising. Retrieved from Johnston et al. (2014).

At the SIT, the rate of GIA in the area has not been applied to the elevation data so the pattern currently follows the patterns seen at a rate of GIA of zero cm/century and parts of the pattern can be seen within both the East and West strandplains. Starting in the most landward side of the West strandplain the pattern begins with a rising followed by a leveling, a lowering and then a final leveling compared to the East strandplain's pattern starting at the most landward ridges begins at the lowering trend and ends with a leveling by Lake Superior. If the East and West strandplain lowering trends were put together it would show the pattern seen in Figure 17 at a rate of GIA of zero.

5.7 Determining Discontinuities Within the Strandplain Data

Once the lakeward and landward segments of the East and West strandplains were determined it allowed for the common pattern and trend at a GIA rate of zero cm/century and the width of the lakeward and landward sections to be used to align the two curves. Using the common pattern and trend, and the width of the lakeward and landward sections of ridges helped decide that the landward set of points of the West strandplain preserved older ridges better than the East strandplain which preserved younger ridges better. Since both the West and East strandplain data contains a lowering within the landward section, the lowering trend will be used to align the two datasets together using similar elevations.

To create one representative curve, the lowering of the West strandplain was aligned to the lowering of the East strandplain by choosing points on the trend that have similar elevations and moving the West strandplain point to the same distance. For the two curves to create one curve representative of the SIT, matching of points with similar trend and elevation was completed twice. The first points that were matched were for the elevation of 182.71 meters at a distance of 102.5 meters on the West strandplain to a distance of 296.5 meters with the same elevation on the East strandplain. Matching the distance of the two points shifted the distance of all the points in the West strandplain data at 102.5 meters and landward by 194 meters. The second set of points that were matched were for the elevation of 183.81 meters at a distance of 132.5 meters on the West strandplain to match 360.5 meters on the East strandplain. The second match resulted in moving the West strandplain point at 183.31 and all subsequent landward points 34 meters farther inland. Once the two points were matched and the discontinuity distances added,

it resulted in the two lowering trends matching as seen in Figure 18. The resulting dataset would then be used to determine a paleohydrograph pattern.

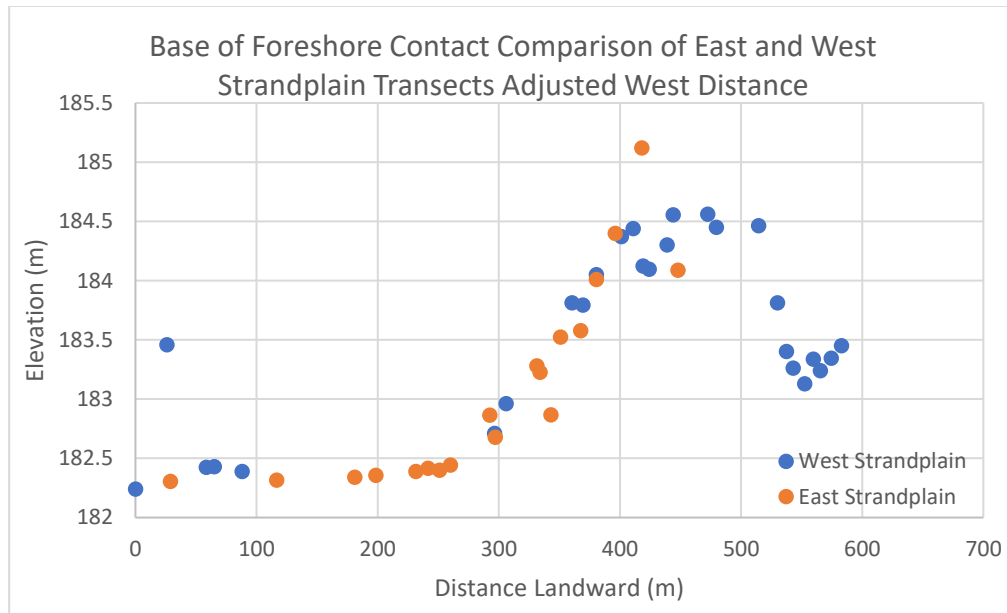


Figure 18 Adjusted distances of the elevations for the base of the foreshore contact of the East and West Strandplains. The West strandplain points were adjusted for discontinuities to form the pattern. The points were adjusted 194 meters for point 102.5 meters and landwards as well as an extra 34 meters for point 132.5 meters and landwards. Two possible outliers are seen at 26 meters and 418 meters.

5.8 Representative Stockton Island Tombolo Elevation Pattern

Prior to being able to compare the adjusted elevation and distance data it must first be made into a common pattern so it can be compared to previously reconstructed paleohydrographs. The common pattern will have the distance data in sequential order to create a line between the points as well as determine any potential outliers within the sequence.

After the distance had been adjusted for the discontinuity, the points for both the West and East strandplains were put together. The data was then sorted by the distance from smallest number (closest to the lake) to the largest number (farthest inland) and expanding the sort area to include the elevation column as well so the elevation stayed with its corresponding distance.

This helped identify the pattern for the SIT inferred paleohydrograph. Since the lakeward data is likely to be younger than the older landward data, the two segments will have their ages determined separately from each other.

Two points were determined to be outliers of the general pattern and were removed from the curve which are points 26 meters distance at 183.46 meters elevation and 418 meters distance at 185.12 meters elevation. The determination of the outliers was by the two points deviating from the pattern that the other points were following. A potential cause for these two outliers could be missing ridges within the sequence where a lowering and rising trend could be occurring but is not present with the existing ridges. Once the outliers were removed the SIT pattern was able to be compared to other paleohydrograph patterns.

5.9 Determination of Potential Age

The exact age of the ridges cannot be determined without fieldwork but the approximate age relative to the millennial lake level phase in the upper Great Lakes (Johnston et al., 2012) can be determined. Millennial phases can be determined in two different ways, either comparing to previously reconstructed paleohydrographs for Lake Superior strandplains using knowledge of patterns and rates of GIA, or through geomorphic characteristics.

The SIT inferred paleohydrograph pattern was compared to the previously constructed paleohydrographs for Lake Superior (Johnston et al., 2012) as seen in Figure 19. Since GIA has been applied to the paleohydrograph curves from Johnston et al. (2012) and not to the inferred paleohydrograph curve at the SIT then knowing how GIA has influenced the curves is important to estimating a potential age from millennial phases. Using Figure 20, it is possible to get estimated rates of GIA for each site based on water gauge data (Mainville and Craymer, 2005).

The lowest rate of GIA for the previously reconstructed paleohydrographs is for Au Train Bay with a rate of negative 12 cm/century which is still much higher than the rate at SIT which is negative 21 cm/century. Patterns seen in Figure 17 show that a lower rate of GIA will have a pattern that has a lower corrected elevation than a rate that is higher than it. Since the SIT has experience a lower rate of GIA compared to the other strandplains around Lake Superior (Johnston et al., 2012), the pattern at SIT should plot below the other paleohydrographs.

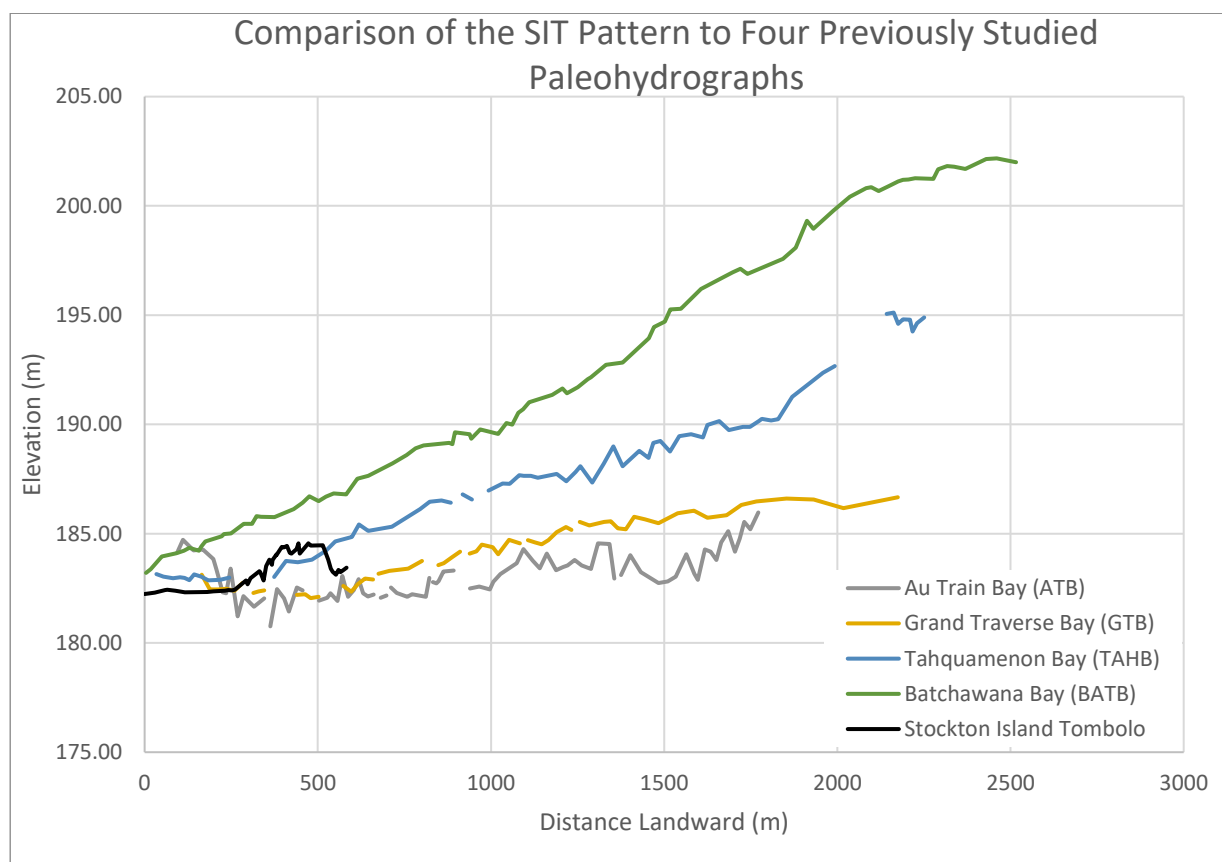


Figure 19 Comparison of the Stockton Island Tombolo paleohydrograph pattern to previously reconstructed paleohydrograph patterns by distance landward. The lakeward segment of the pattern at SIT is below the four different curves while the landward segment at SIT is mainly above the other paleohydrographs. To fit with the known rates and patterns of GIA in Lake Superior, the landward segment of the SIT needs to move to the right by at least 1,800 meters to be below all other paleohydrograph curves. Paleohydrograph data was retrieved from Johnston et al. (2012).

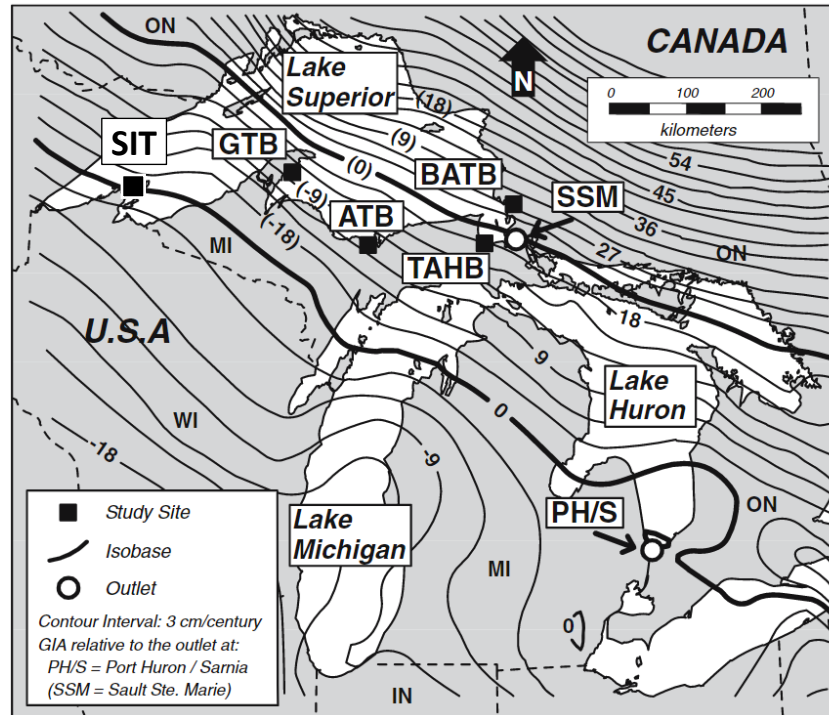


Figure 20 Glacial isostatic adjustment (GIA) derived from water-level gauge data with previously reconstructed paleohydrograph study locations. The two outlets shown on the map are Port Huron and Sarnia (PH/S) and Sault Ste. Marie (SSM). Relating the rate of GIA to the SSM outlet the rates are 6 cm/century for Batchawana Bay (BATB), 3 cm/century for Tahquamenon Bay (TAHB), -7.5 cm/century for Grand Traverse Bay (GTB), -12 cm/century for Au Train Bay (ATB), and -21 cm/century for the Stockton Island Tombo (SIT). Modified from Johnston et al. (2007).

Using the locations of the previous reconstructed paleohydrograph as well as knowing older ridges are located farther landward; the SIT inferred paleohydrograph pattern can be moved horizontally along the x-axis to determine a potential millennial phase of both the lakeward and landward sections. At the current location of the lakeward section in Figure 19, the ridges all plot lower than the other curves placing it approximately in the Sub-Sault phase. For the landward ridges, it does not fall underneath the curve at its current location, so it needs to be moved farther along the x-axis. When moving it along the x-axis, all the landward ridges are underneath the paleohydrographs when the most lakeward point of the landward sequence is at approximately 1,800 meters. Moving the start of the landward section to the distance of 1,800 meters inland will place the section into the Nipissing millennial phase.

The approximate age of the lakeward ridges is also supported by geomorphic data seen by two features on the East strandplain's lakeward section. These two features often correlate to the change of the active outlet from Port Huron/Sarnia to SSM that occurred approximately 1,060 years ago (Johnston et al., 2007 and 2012). These two features are sloughs that are filled with water and the large bend in the creek (Johnston et al., 2007) seen in Figure 21 which is a satellite image of the SIT. Both the bend in the creek as well as the sloughs begin to occur around the same ridge meaning that the two features most likely formed around the same time as the ridge. Since the bend in the creek and slough occur in the middle section of the lakeward section of the East strandplain then 1,060 years ago is possibly the age for the middle of the lakeward segment.



Figure 21 Geomorphic evidence on the Stockton Island Tombolo supporting age estimate of lakeward ridges. Sloughs and bend of the creek marked on the image have been related to the change of the active outlet of Lake Superior approximately 1,060 years ago (Johnston et al., 2007).

Other data supporting the age of the landward ridges is the maximum elevation of the Nipissing phase from the Port Huron/Sarnia paleohydrograph is 183.3 meters (Thompson et al., 2014). When comparing to the maximum elevation of the SIT inferred paleohydrograph pattern the highest point in the landward segment is approximately 184.6 meters. The rate of GIA does not have to be adjusted between the two sites because as Figure 20 shows, the location of Port Huron/Sarnia is at the same rate of GIA as the SIT. Since both elevations are relatively close to each other and the rate of GIA should be the same, it can be assumed that the highest elevation on SIT correlates with the peak of the Nipissing phase.

5.10 Age Determination Using the Sault Ste. Marie Outlet Paleohydrograph

To estimate the age for the inferred SIT paleohydrograph reconstructed in this thesis from topographic data and a correction factor, present day elevations in paleohydrographs reconstructed using field coring and age-dating techniques completed for other Lake Superior strandplains are needed for comparison. However, ancient shorelines of similar age in different strandplains around Lake Superior are at different elevations than the SIT. To compare elevations, one needs to account for GIA to help estimate an age for the ridges of the SIT. Since the outlet for Lake Superior changed through time, the relationship of vertical ground movement at the active outlet which helps to regulate the water plane in the lake and ground surface elevation at the SIT needs to be accounted for. The active outlet in today's Lake Superior is the SSM outlet and so the SIT was compared to the SSM outlet paleohydrograph reconstructed in Johnston et al. (2012). The SSM outlet could be considered to have a relative GIA rate of zero since it currently helps to regulate the Lake Superior basin water plane. But because the rates of GIA vary, a few simple approaches were attempted to estimate a general age of the SIT ancient shorelines.

The SSM outlet paleohydrograph was used as a reference to interpret the SIT because ages were assigned to the SSM outlet paleohydrograph so it could help approximate the age ranges of lakeward and landward ridges at SIT. Three different potential rates of GIA were chosen to estimate the approximate age of SIT using GIA. The three rates of GIA chosen were 15, 21, and 33 cm/century and were derived from geological knowledge of ancient shorelines in strandplains (Johnston et al., 2012) and instrumental water-level gauge records (Mainville and Craymer, 2005).

To determine potential ages from the GIA adjusted SSM outlet paleohydrograph, the trends and elevations were considered when deciding what age the ancient shorelines in SIT could be. Both elevation and trend were used together to determine where the SIT curve would fit the best or align with the GIA adjusted SSM outlet paleohydrograph. Firstly, the elevation would be considered to find potential locations that could work on the adjusted SSM outlet paleohydrograph. Then the trend of the pattern would help to better align the curves. Considering that most likely there are missing data points within the SIT inferred paleohydrograph pattern, the overall trend and not the individual lowering and rises were taken into consideration. From the most landward ridge towards the lakeward ridges the overall trend of the landward segment is a rising, a leveling followed by a lowering while the overall trend for the lakeward segment is a leveling. To determine the ages of the ridges at SIT, the inferred paleohydrograph pattern will be determined based on the lakeward and landward ridges. To align the SIT inferred paleohydrograph data along the curve of the SSM outlet paleohydrograph an equal rate of 30 years was applied to each ridge no matter the distance between the ridges. To determine the starting age for the SIT inferred paleohydrograph pattern, the overall trend and

elevation were matched to the adjusted SSM outlet paleohydrograph curve first keeping the age spacing the same.

The first rate of GIA chosen was based on the water-level gauge records (Figure 20), where the rate of GIA of the SIT is negative 21 cm/century and was applied to the SSM outlet paleohydrograph (Mainville and Craymer, 2005). After aligning the elevation of the inferred SIT paleohydrograph pattern to the adjusted SSM outlet paleohydrograph, the starting age for the lakeward and landward sections were 440 years and 2,640 years, respectively. The resulting comparison, Figure 22, placed the lakeward section of the SIT inferred paleohydrograph pattern in the Sub-Sault phase while it placed the landward section between in the Nipissing to Algoma phases. From the potential millennial phase ages that were determined earlier, this rate of GIA correlates with the lakeward ridges potential age and is near the end of the potential millennial phase for the landward ridges.

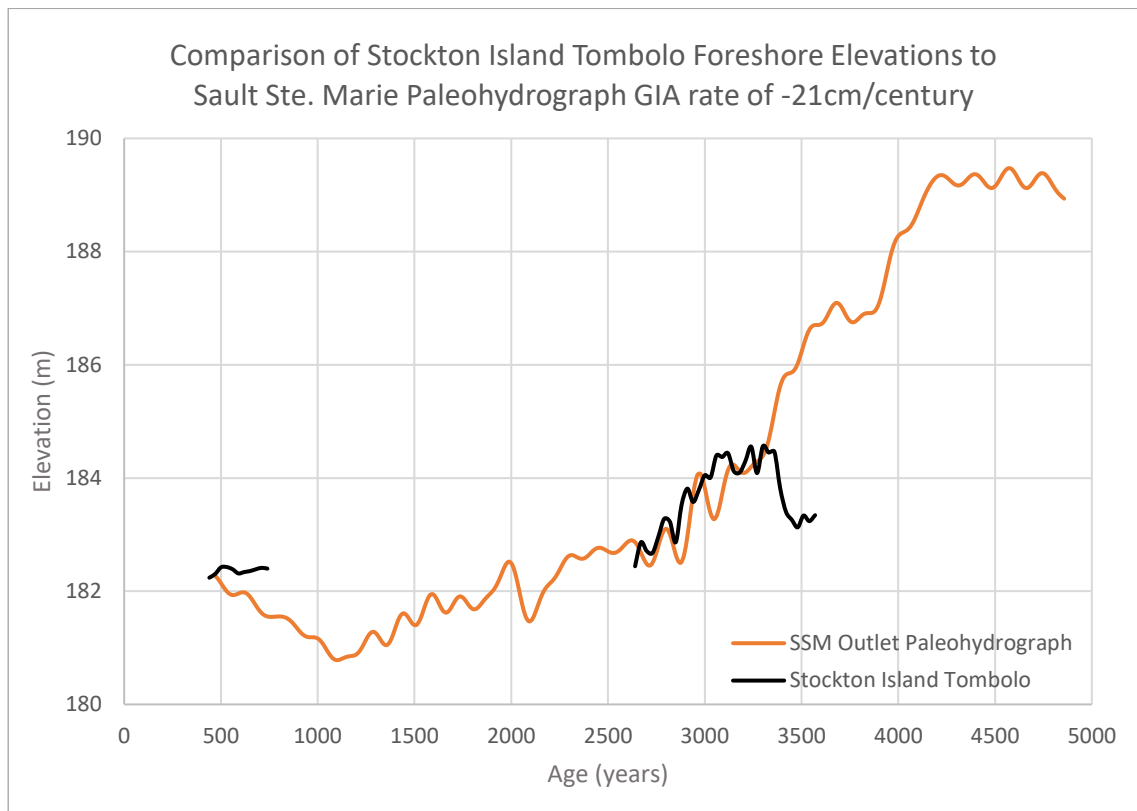


Figure 22 Glacial isostatic rebound adjusted Sault Ste. Marie paleohydrograph compared to the Stockton Island Tombolo pattern. Rate of GIA of negative 21 cm/century aligning the elevations of the landward and lakeward ridges being Nipissing to Algoma phases and Sub-Sault phase, respectively. Sault Ste. Marie outlet paleohydrograph data retrieved from Johnston et al. (2012).

The second rate of GIA is negative 15 cm/century, which was chosen because it was found in Johnston et al. (2012) that GIA calculated by water-level gauge records does not always match the GIA found through coring of strandplains. It was found that the studied strandplains around Lake Superior either have the same rate of GIA as the water-level gauge records or the water-level gauge GIA is off by approximately 6 cm/century (Johnston et al., 2012). The rate of GIA found from the water-level gauge records (21 cm/century) was then adjusted by the 6 cm/century to determine the rate of GIA of negative 15 cm/century. After aligning the elevation of the inferred SIT paleohydrograph pattern to the adjusted SSM outlet paleohydrograph, the starting age for the lakeward and landward sections were 460 years and 2,030 years,

respectively. The resulting comparison seen in Figure 23 aligned the lakeward section of the inferred SIT paleohydrograph pattern in the Sub-Sault phase while the landward section was placed in the Algoma phase. Comparing the results with the potential phase millennial phase ages, the lakeward ridges are in a similar millennial phase as predicted, but the millennial phase for the landward ridges is younger than the Nipissing phase.

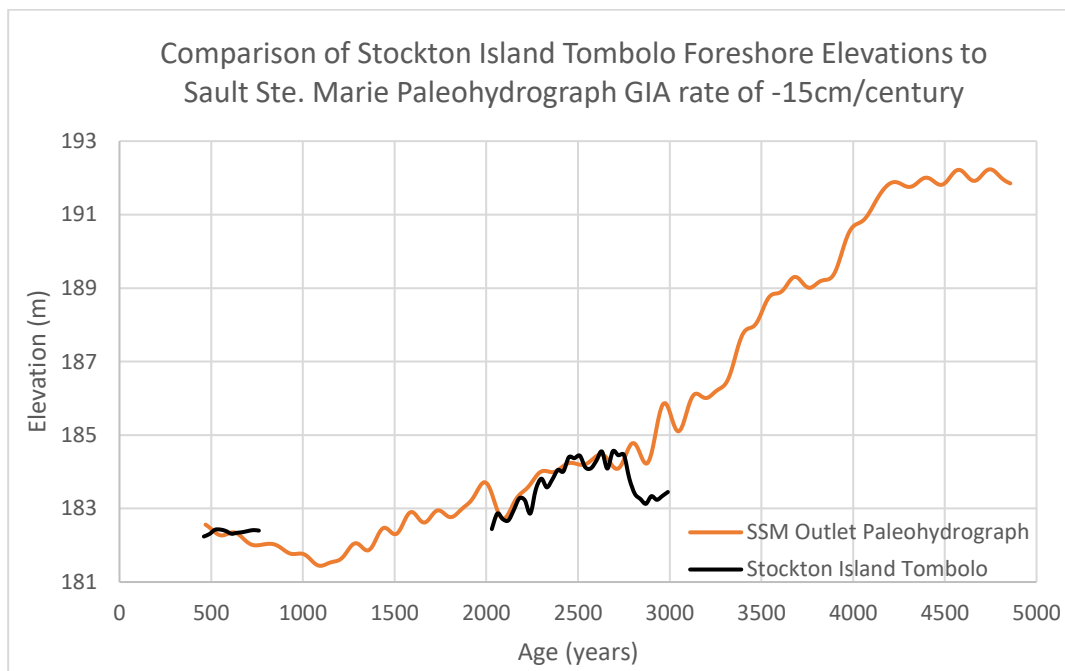


Figure 23 Glacial isostatic rebound adjusted Sault Ste. Marie paleohydrograph compared to the Stockton Island Tombolo pattern. Subtracting a rate of GIA of 15 cm/century aligning the elevation of the landward and lakeward ridges approximately in the Algoma and Sub-Sault phases, respectively. Sault Ste. Marie outlet paleohydrograph data retrieved from Johnston et al. (2012).

The third rate of GIA is negative 33 cm/century is based on a study where the paleohydrograph of Ipperwash (Morrison, 2017) that is located near the Port Huron/Sarnia outlet was related to the SSM outlet and subtracting a rate of GIA of 33 cm/century brought the two paleohydrograph curves the closest together (Johnston et al., 2012). When matching the trend and elevation of the SSM outlet paleohydrograph and the inferred SIT paleohydrograph pattern, only the landward section was matched since the lakeward section would have been placed in

the Nipissing which does not match the potential millennial phase. The starting age for the landward ridges was 3,740 years. The resulting comparison of the inferred SIT paleohydrograph and the SSM outlet paleohydrograph seen in Figure 24 placed the landward section into the Nipissing phase which is also the potential millennial phase for the landward ridges.

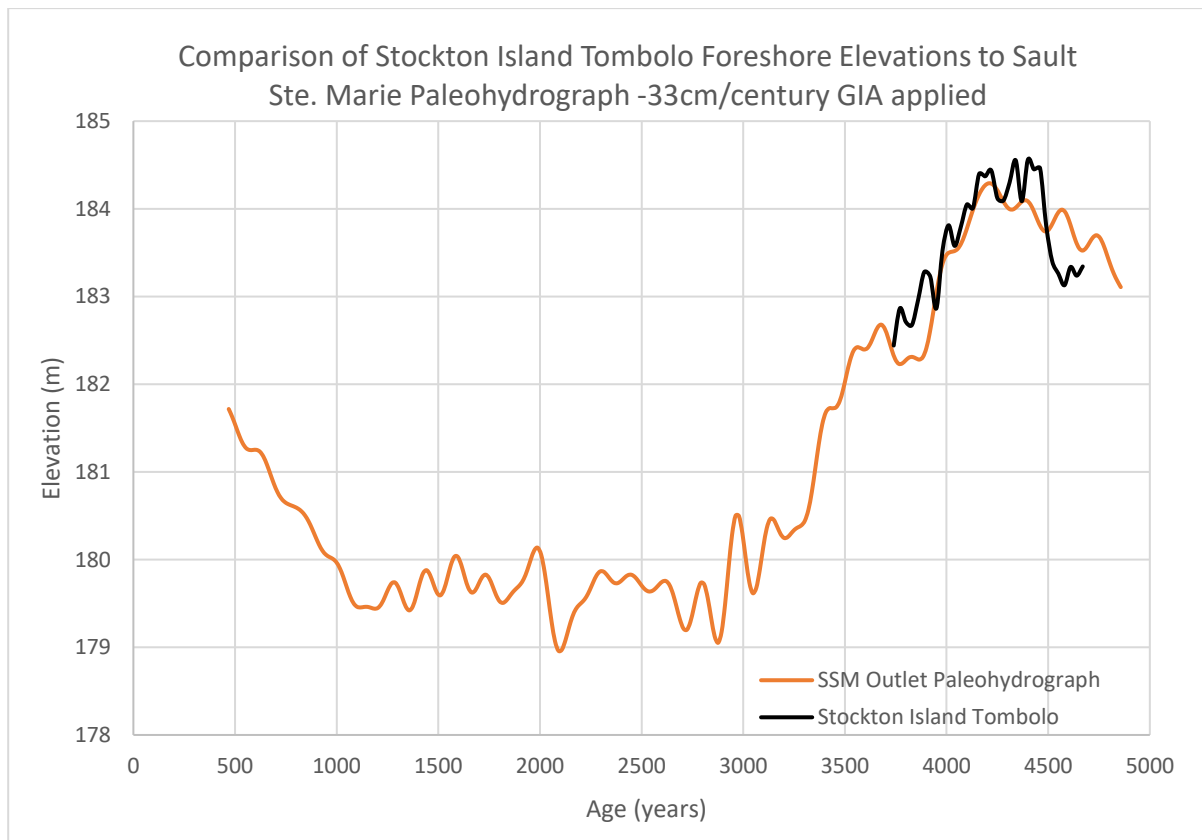


Figure 24 Glacial isostatic rebound adjusted Sault Ste. Marie paleohydrograph compared to the Stockton Island Tombolo pattern. Rate of GIA of negative 33 cm/century aligning the elevation of the landward ridges to be in the Nipissing phase. Sault Ste. Marie outlet paleohydrograph data retrieved from Johnston et al. (2012).

The approximate resulting ages, seen in Table 3, for a GIA of negative 15 cm/century from the SSM outlet paleohydrograph is the lakeward ridges are in the Sub-Sault phase, 460 to 760 years ago, and the landward ridges are in the Algoma phase being 2,030 to 2,990 years ago. For a GIA rate of negative 21 cm/century from the elevation the lakeward ridges are in the Sub-Sault phase, 440 to 740 years ago, while the landward sediments are between the Algoma and

Nipissing phases and are aged 2,640 to 3,600 years ago. Finally, for a rate of GIA of negative 33 cm/century the estimated the age of the landward ridges in the Nipissing phase for the age range of 3,740 to 4,700 years ago.

Table 3 Inferred ages determined by matching the inferred Stockton Island Tombolo paleohydrograph to the Sault Ste. Marie outlet paleohydrograph. Ridge number represents the location of the ridge in Figure 18 without the two determined outliers. The most lakeward ridge is 1 while the most landward ridge is 44. For both the landward and lakeward sections the ages increase as the rate of GIA becomes more negative.

	Ridge Number	Strandplain	Distance (m)	Elevation (m)	Rate of GIA -15cm/century Age (Years)	Rate of GIA -21cm/century Age (Years)	Rate of GIA -33cm/century Age (Years)
Lakeward Ridges	1	West	0	182.24	460	440	-
	2	East	29	182.30	490	470	-
	3	West	58.5	182.42	520	500	-
	4	West	65	182.43	550	530	-
	5	West	88	182.39	580	560	-
	6	East	116.5	182.31	610	590	-
	7	East	181	182.34	640	620	-
	8	East	198.5	182.36	670	650	-
	9	East	231.5	182.39	700	680	-
	10	East	241.5	182.41	730	710	-
	11	East	251	182.40	760	740	-
Landward Ridges	12	East	260	182.44	2030	2640	3740
	13	East	292.5	182.86	2060	2670	3770
	14	West	296.5	182.71	2090	2700	3800
	15	East	297	182.68	2120	2730	3830
	16	West	306	182.96	2150	2760	3860
	17	East	331.5	183.28	2180	2790	3890
	18	East	334	183.23	2210	2820	3920
	19	East	343	182.87	2240	2850	3950
	20	East	351	183.52	2270	2880	3980
	21	West	360.5	183.81	2300	2910	4010
	22	East	367.5	183.58	2330	2940	4040
	23	West	369.5	183.79	2360	2970	4070
	24	West	380.5	184.05	2390	3000	4100
	25	East	380.5	184.01	2420	3030	4130
	26	East	396	184.40	2450	3060	4160
	27	West	401	184.37	2480	3090	4190
	28	West	411	184.44	2510	3120	4220
	29	West	419	184.12	2540	3150	4250
	30	East	424	184.10	2570	3180	4280
	31	East	439	184.30	2600	3210	4310
	32	East	444	184.55	2630	3240	4340
	33	East	448	184.09	2660	3270	4370
	34	West	472.5	184.56	2690	3300	4400
	35	West	479.5	184.45	2720	3330	4430
	36	West	514.5	184.46	2750	3360	4460
	37	West	530	183.81	2780	3390	4490
	38	West	537.5	183.40	2810	3420	4520
	39	West	543	183.26	2840	3450	4550
	40	West	552.5	183.13	2870	3480	4580
	41	West	559.5	183.34	2900	3510	4610
	42	West	565.5	183.24	2930	3540	4640
	43	West	574.5	183.34	2960	3570	4670
	44	West	583	183.45	2990	3600	4700

The rate of GIA of negative 33 cm/century placed the landward segments in the correct millennial phase where the highest point related to the peak of the Nipissing phase. The pattern of the landward segments also relates better since looking at both from the oldest to youngest ridges has a rise, a short leveling, and a final lowering phase. By using the age range from the rate of GIA of negative 33 cm/century, the approximate ages of the landward ridges are around 3,740 to 4,700 years ago. As for the lakeward segment, GIA rates of negative 15 and 21 cm/century placed the ridges in the Sub-Sault phase where the age range is between 440 to 730 years ago. Since SIT is at a zero isobase with the Port Huron/Sarnia outlet (Figure 20), the highest elevation of the Nipissing at this location can be used to compare the SIT inferred paleohydrograph pattern. The peak of the Nipissing at Port Huron/Sarnia is 183.3 meters (Thompson et al., 2014) and the inferred SIT paleohydrograph pattern the peak is 184.6 meters. Since both areas are located on the same isobase they should have the same elevation, which could mean that the correction factor used could be incorrect.

5.11 Validity of the Method

The validity of this new method that is the first application of Heather (2021) used in this thesis will not fully be known until subsurface coring and age dating is completed for SIT. The most accurate method to reconstruct a paleohydrograph from ancient shorelines in the Great Lakes strandplains requires fieldwork (Johnston et al., 2014). These field methods involve retrieving the subsurface elevation of the base of the foreshore contact (a proxy for ancient lake level) and digging soil pits to age-date sediments using OSL dating. Once fieldwork has been completed, the paleohydrograph that is reconstructed can be compared to the inferred paleohydrograph created in this thesis to determine if this new method is a viable alternative to reconstruct paleohydrographs in remote locations or before fieldwork begins. If it is not deemed

accurate more work should be completed to compare how topographic and subsurface elevations in strandplains at different locations at different times compare.

5.12 Sources of Error

Without currently knowing the validity of the method used to determine the inferred paleohydrograph, sources of error can only be speculated as to what they may be. Three areas within the method that may affect the resulting ages found are the chosen location of the transect, the correction factor, and the rate of GIA used.

The chosen location of the transect could be a potential source of error as it was completed by going through the data and finding what appeared to be the best transect location. Since this was done by hand and not through a sequential algorithm by a computer program there is a likelihood that an appropriate transect may not have been chosen due to human error or bias. If the transect chosen was not the most representative of its respective strandplain then the topographic swale elevation may also be different since the swale and ridge elevations changed between transects of the same strandplain. Distance between ridges also changed between transects as some transects had a smaller distance for the lakeward section that caused a larger distance for the landward section which could change the number of ridges divided between the lakeward and landward sections.

The correction factor could be another source of error. If the correction factor is incorrect, it would cause the elevation to be higher or lower than the elevations used to determine the ages. If the correction factor is determined to be smaller than the 1.49 meters used, then the elevation used to determine age would be an underestimation causing the determined age to also be an underestimation of the actual age. On the other hand, if the correction factor is larger than the

1.49 meters used then it would cause the data used in this thesis to be an overestimation of elevation and age. Considering the Port Huron/Sarnia paleohydrograph elevation for the peak of the Nipissing was found to be 183.3 meters (Thompson et al., 2014) and the highest point of the SIT inferred paleohydrograph pattern was 184.6 meters it could possibly mean the correction factor was underestimated. The correction factor could also vary for each ridge since the distance between the topographic elevation and the base of the foreshore subsurface contact elevation varies between ridges when data is collected in the field (Johnston et al., 2014). To help avoid using one constant correction factor for all topographic elevations, potentially ridges could be grouped together, and a different correction factor could be used for each group of ridges or each ridge could have its own unique correction factor.

The rate of GIA is another potential factor that could cause an over or under estimation of the age of all ridges. The rates of GIA chosen for this thesis were dependent upon interpretations from varied geological information (Johnston et al., 2012) and instrumental water-level gauge records (Mainville and Craymer, 2005). As stated in Johnston et al. (2012), there are some discrepancies between lake basins, especially through time. If the estimated GIA does not remove enough elevation per century, then the age estimates will be lower than what was found. On the other hand, if the GIA rates used in this thesis are removing too much elevation per century, then the ages would be overestimated.

5.13 Erosion and Flooding of the Stockton Island Tombolo

Relative high lake levels in Lake Superior have become a greater concern over their potential to cause erosion and flooding. Extreme events found in paleohydrographic ancient shorelines research (Johnston et al., 2014) reports that we are currently within a relative high

lake level of a natural multi-decadal lake level oscillation that has been persistent for five millennium. So, relative lake levels are currently high and rising and if it stays high and rising over the next few years, it could cause concerns for erosion and flooding at SIT. In the southwestern portion of Lake Superior where AINL is located, it was determined in this thesis through the inferred SIT paleohydrograph that the area is lowering at least by 15 cm/century compared to the SSM outlet of the lake due to GIA. Since the outlet helps to control the water plane of Lake Superior and the ground surface at the outlet is rising more rapidly than at AINL, then that is a concern especially over the long term due to GIA. Oscillations and GIA are two very important components working to increase relative lake levels impacting AINL, particularly the SIT and PBH which are at risk of being eroded and/or flooded.

One way that SIT could possibly be saved naturally is if the rate of sediment supply to the area is faster than the long-term rate of lake level rise (Johnston et al., 2014). A high rate of sedimentation at the current coastline can help protect areas that are inland like the PBH and the bog within SIT. If the rate of sediment supply is slower than the long-term rate of lake level rise, then there will be more erosion occurring along SIT. If all the lakeward ridges and especially the large ridges currently adjacent to Lake Superior become eroded from rising relative lake levels, then inland areas will not have a layer of protection (i.e. the PBH). In both the West and East strandplains of the SIT, there is a large lakeward ridge that ranges between two to four meters above current Lake Superior water levels. And landward of the topographically high ridges is the leveling which has a lower elevation that seems level or nearly horizontal. The elevation of the leveling is approximately the same elevation or a maximum of about 0.3 meters higher than the current water level in Lake Superior and modern coastal sediments. If the relatively large lakeward ridges are eroded away there will be nothing left to protect the area further inland and

especially prevent flooding of the lakeward ridges on SIT. So, the rate of sediment supply is very important for AINL park managers to consider, especially when trying to help protect and preserve the SIT and its unique features such as the PBH.

6.0 Recommendations

Below are several recommendations that help to further expand upon the understanding of erosion and flooding on the SIT as well as ideas to further develop the method used.

- Create a flood map like the ones used by the Federal Emergency Management Agency to predict the damage that different water level elevations will cause.
- Determine the rate of sedimentation as it will determine the amount of erosion protection that will be needed for the SIT.
- If erosion protection is necessary, find a solution that does not impede the rate of sedimentation to allow ridges to build up while also being protected from erosion.
- Determine an accurate rate of GIA for isobases in the upper Great Lakes so if the method is used in the future a value of GIA is known for the study area and can be accurately applied.
- Use the method in Heather (2021) with the other previously studied sites that have been cored and have a reconstructed paleohydrograph to determine if one correction factor can be used for all sites or if the correction factor changes based on location, the isobase, age or shape of the strandplain.

7.0 Conclusion

Over the past few years, the upper Great Lakes have been experiencing an increased lake level causing a greater risk of erosion and flooding. The SIT within Lake Superior protects the PBH from flooding, but there is recent concern that it will be eroded and/or flooded. By reconstructing an inferred paleohydrograph of the SIT allows for a better understanding of the past lake level patterns and trends as well as understanding the ages of the ridges. The method used in this thesis is experimental and takes topographic elevations from LIDAR to estimate the base of the foreshore contact elevation which is then compared to a previously reconstructed paleohydrograph that has GIA applied to it to approximate ages of the ridges. The method was first mentioned in Johnston et al. (2012) and then further developed by Heather (2021), but never done without knowledge from cored ridges until now.

Through this method it was determined that the landward ridges within the SIT are within the Nipissing phase and the ages determined for them are between 3,740 and 4,700 years ago when assuming a rate of GIA of negative 33 cm/century. The lakeward ridges were determined to have formed in the Sub-Sault phase when a rate of GIA negative 15 or 21 cm/century was applied with the ages being between 460 to 760 years ago. The millennial phases for the landward and lakeward ridges was also supported by evidence collected from comparisons of elevation and distance with other paleohydrographs, geomorphic evidence, and the elevation for the peak of the Nipissing. Considering the rate of GIA at the SIT and the increased lake levels from natural oscillation there is a high likelihood that the SIT and PBH will face erosion and flooding.

Though this method is experimental, it has potential to help guide upcoming fieldwork, which in return will determine the viability of this remote paleohydrograph reconstruction at the SIT. Future studies are also needed to further determine if it is possible to accurately reconstruct paleohydrographs for sites that cannot be cored. If proven to be reliable, remote paleohydrographs can help better our understanding of the ancient lake level pattern and trends in the Great Lakes and beyond. Please see Appendix A which includes a broad overview of this thesis and an initial preliminary thesis design presented in posters.


8.0 References

- Baedke, S.J. & Thompson, T.A. (2000). A 4,700-year record of lake level and isostasy for Lake Michigan. *Journal of Great Lakes Research*, 26(4), 416-426. doi: 10.1016/S0380-1330(00)70705-2
- Brock, J. C., & Purkis, S. J. (2009). The emerging role of LIDAR remote sensing in coastal research and resource management. *Journal of Coastal Research*, 10053(6), 1-5. doi:10.2112/SI53-001.1
- Cary, S. J., McDowell, P. F., & Graumlich, L. J. (1979). Soil and surficial geology of four Apostle Islands. *Wisconsin Academy of Sciences, Arts and Letters*, 67, 15-40.
- Esri Inc. (2020). *ArcGIS Pro* (Version 2.5). Esri Inc. <https://www.esri.com/en-us/arcgis/products/arcgis-pro>.
- Heather, M. (2021). *Comparing paleohydrograph reconstructions from subsurface stratigraphy and topography at the Sault Ste. Marie strandplain*. (Undergraduate thesis, University of Waterloo, Waterloo, Canada)
- Huff, M. G. (2019). A high-resolution paleoecological perspective on historical fire regimes in Great Lakes barren communities of Stockton Island, Wisconsin. (Lehigh University).
- Johnston, J. W., Argyilan, E. P., Thompson, T. A., Baedke, S. J., Lepper, K., Wilcox, D. A., et al. (2012). A Sault-outlet-referenced mid- to late-Holocene paleohydrograph for Lake Superior constructed from strandplains of beach ridges. *Canadian Journal of Earth Sciences*, 49(11), 1263-1279. doi:10.1139/e2012-057
- Johnston, J. W., Thompson, T. A., & Wilcox, D. A. (2014). Palaeohydrographic reconstructions from strandplains of beach ridges in the Laurentian Great Lakes. *Geological Society Special Publication*, 388(1), 213-228. doi:10.1144/SP388.22
- Johnston, J., Thompson, T., Wilcox, D., & Baedke, S. (2007). Geomorphic and sedimentologic evidence for the separation of Lake Superior from Lake Michigan and Huron. *Journal of Paleolimnology*, 37(3), 349-364. doi:10.1007/s10933-006-9052-3
- Joyce, K. (2019a, April 9). *Creating and Editing Feature Classes in ArcGIS Pro* [Video]. YouTube. <https://www.youtube.com/watch?v=gXjMDL3NgRA&t=311s>
- Joyce, K. (2019b, April 8). *Creating Feature Classes in ArcGIS Pro* [Video]. YouTube. <https://www.youtube.com/watch?v=L2hmTvSEK0c>
- Kerfoot, W. C., Hobmeier, M. M., Green, S. A., Yousef, F., Brooks, C. N., Shuchman, R., et al. (2019). Coastal ecosystem investigations with LiDAR (light detection and ranging) and bottom reflectance: Lake Superior reef threatened by migrating tailings. *Remote Sensing (Basel, Switzerland)*, 11(9), 1076. doi:10.3390/rs11091076

- Mainville, A., & Craymer, M. R. (2005). Present-day tilting of the Great Lakes region based on water level gauges. *Geological Society of America Bulletin*, 117(7), 1070. doi:10.1130/B25392.1
- Morrison, S., & Johnston, J. (2017). *Natural Late Holocene lake level fluctuations recorded in the Ipperwash strandplain, southern Lake Huron*. University of Waterloo.
- National Park Service. (2011). *General management plan / wilderness management plan for Apostle Islands National Lakeshore summary document* US National Park Service.
- Nichols, G. (2009). *Sedimentology and stratigraphy* (2nd ed.). Wiley-Blackwell.
- O'Neil-Dunne, J. (2019, January 6). *LiDAR Surface Models in ArcGIS Pro* [Video]. YouTube. <https://www.youtube.com/watch?v=L4tVXARSrUo>
- Otvos E.G. (2017) Beach Ridges. In: Finkl C., Makowski C. (eds) Encyclopedia of Coastal Science. Encyclopedia of Earth Sciences Series. Springer, Cham. doi: 10.1007/978-3-319-48657-4_39-2
- Owens E.H. (1982) Tombolo. In: Beaches and Coastal Geology. Encyclopedia of Earth Sciences Series. Springer, New York, NY. doi:10.1007/0-387-30843-1_474
- Pendleton, E. A., Thieler, E. R., & Williams, S. J. (2007). *Coastal change-potential assessment of Sleeping Bear Dunes, Indiana Dunes, and Apostle Islands National Lakeshores to lake-level changes*. Reston, Va: U.S. Geological Survey. Retrieved from <http://purl.access.gpo.gov/GPO/LPS89685>.
- Thompson, T. A., Johnston, J. W., & Lepper, K. (2014). *The contemporary elevation of the peak Nipissing phase at outlets of the upper Great Lakes*. Geological Society of America. doi: 10.1130/2014.2508(02).
- Thornberry-Ehrlich, T. L. (2015). *Apostle Islands National Lakeshore: Geologic resources inventory report*. Fort Collins: Natural Resource.
- United States Army Corps of Engineers [USACE]. (2020). Great Lakes Water Levels (1918-2020). [PDF]. Retrieved from: <http://lre-wm.usace.army.mil/ForecastData/GLBasinConditions/LTA-GLWL-Graph.pdf>
- U.S. Geological Survey, National Geospatial Technical Operations Center, 2019 03 25, USGS Topo Map Vector Data (Vector) 43276 Stockton Island, Wisconsin 20190325 for 7.5 x 7.5 minute FileGDB 10.1: U.S. Geological Survey.
- Wisconsin Department of Natural Resources. (2017). Bayfield Co. QL2 LiDAR (2015-16) - Classified Point Cloud (2). [Data file]. Retrieved from <https://coast.noaa.gov/dataviewer/#/lidar/search/where:id=6337>.

Appendix A

Poster presentation for the initial thesis design.



UNIVERSITY OF WATERLOO

Palaeohydrograph Reconstruction for the Stockton Island Tombolo

Dayna Opersko
Department of Earth and Environmental Science
University of Waterloo

Abstract

Rising lake levels have become a concern for the coasts of Lake Superior and one such coastline is the Stockton Island Tombolo that protects the Pine Barrens Habitat in the Apostle Islands National Lakeshore (AINL), Wisconsin, U.S.A. If the Stockton Island Tombolo is lost the threatened and endangered species will disappear. For the AINL, managers to make an informed decision on how to protect this unique and sensitive area, they need to understand how lake level and coastal sediments will change. Lake level trends and patterns for Lake Superior have been reconstructed from ancient preserved shorelines, creating palaeohydrographs that help to understand how lake level has changed in the past (Johnston et al., 2012). Though fieldwork has been postponed until Summer 2021 due to COVID-19, there is an opportunity to apply a method mentioned in Johnston et al. (2012) that uses topographic elevation and a correction to reconstruct a palaeohydrograph from the shorelines at AINL. This new AINL palaeohydrograph can potentially help guide fieldwork for the summer of 2021.

Context

Apostle Islands National Lakeshore

- Shoreline have been completed at AINL but mainly focus on plants and animals
- Research has been completed and have found that the Stockton Island Tombolo has a very high change potential (Figure 2) (Pondellon et al., 2007)
- The park has a management plan that states sandscapes are allowed to go through erosion and deposition but the real issue is protecting the Pine Barrens Habitat that the National Park Service, which includes AINL, has a mandate to preserve and protect (National Park Service, 2011)
- The Pine Barrens Habitat is home to threatened and endangered species that the parks management plan states that they are required to conserve and protect the species from being lost (National Park Service, 2011)
- Expertise about lake level fluctuations and their impact on AINL coastal systems needed to better understand the potential of erosion and flooding

Palaeohydrographic Research

- A research group has reconstructed lake levels for the past six millennium in the upper Great Lakes (Johnston et al., 2014)
- AINL shorelines has not been studied by the research group but they have conducted many studies of ancient shorelines around Lake Superior and one for the Lake Superior outlet (Johnston et al., 2014)
- Palaeohydrographs are created collecting cores to obtain surface elevation data from lacustrine ridges in the Laurentian Shield and sediment through optically stimulated luminescence (OSL) (Johnston et al., 2014)
- In Johnston et al. (2012) an idea is mentioned that uses topography and a correction factor to reconstruct a palaeohydrograph for a site that has never been cored

Topographic Elevation - Lidar

- Lidar is the most accurate remote sensing data for elevation (Brook & Purkis, 2009)
- Lidar can go through foliage and allow the topographic elevation to be retrieved (Brook & Purkis, 2009)

Glacial Isostatic Adjustment (GIA)

- The process of GIA causes vertical elevation changes through time and affect the elevation results and interpretations
- Rates of GIA have been published using geotopical data from Lake Superior palaeohydrographs (Johnston et al., 2012)
- Rates of GIA were published using historical water level gauge data. The direction and amount of vertical change can be estimated for AINL (Figure 3) (Manville & Craymer, 2005)

References

Brook, J. C., & Purkis, S. J. (2009). The emerging role of lidar remote sensing in coastal research and resource management. *Journal of Coastal Research*, 10(25)(6), 1-15. doi:10.2112/1053-9101.1053.9101.1

Huff, M. G. (2010). A high-resolution palaeogeographic perspective on historical fire regimes in Great Lakes basins: communities of Stockton Island, Wisconsin. *Lehigh University*.

Johnston, J. W., Argallan, E. P., Thompson, T. A., Backus, S. J., Lepper, K., Wilcox, D. A., et al. (2012). A multi-core referenced model to lake Superior palaeohydrograph for lake superior reconstructed from strandplains of beach ridges. *Canadian Journal of Earth Sciences*, 49(11), 1263-1279. doi:10.1139/cjes12-012-057

Manville, A., & Craymer, M. R. (2005). Present-day tilting of the Great Lakes region based on water level gauges. *Geological Society of America Bulletin*, 117(7), 1079. doi:10.1130/B25392.1

National Park Service. (2011). *Current management plan / wilderness management plan for apostle islands national lakeshore summary document* US National Park Service.

Pondellon, E. A., Thiesler, E. R., & Williams, S. J. (2007). Coastal change-potential assessment of sleeping bear-dunes, inland dunes, and apostle islands national lakeshores to 1000-year level changes. Reston, Va: U.S. Geological Survey. Retrieved from <http://pubs.usgs.gov/of/2007/OLFS89/858/>

Introduction

Rising lake levels cause flooding and erosion in the Upper Great Lakes and threaten protected areas and habitats of endangered species. Managers of national parks need help from researchers to understand the severity of erosion and flooding possible. The study site for this thesis is located at AINL on Lake Superior in Wisconsin, United States. One of the islands in the park, Stockton Island, is connected to Presque Isle by a coastal feature called a tombolo, the Stockton Island Tombolo (Figure 1). The Pine Barrens Habitat occurs on the Stockton Island Tombolo which helps to protect this unique habitat that is home to endangered plants and animals. If water levels in Lake Superior remain high or rise more that will lead to more flooding and erosion of the Stockton Island Tombolo and further threaten the Pine Barrens Habitat. Restrictions caused by COVID-19 has halted field research for the Stockton Island Tombolo by Great Lakes coastal experts, but allows for an opportunity to research the tombolo remotely using data published by coastal experts in Lake Superior-shoreline research.

Figure 1 Location of Stockton Island Tombolo.

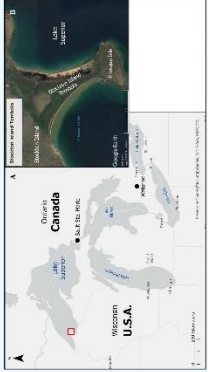


Figure 1 shows the location of Stockton Island Tombolo in the Great Lakes region. (A) shows the location of the tombolo connecting Stockton Island to Presque Isle. (B) shows the location of the tombolo connecting Stockton Island to Presque Isle.

Figure 2 Relative Coastal Change Potential of Apostle Islands National Lakeshore.

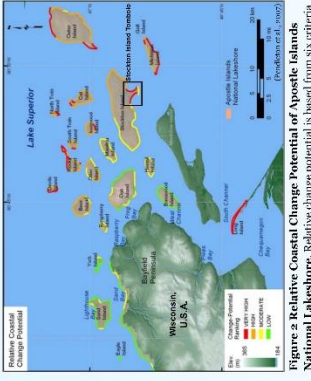


Figure 2 is a map of the Apostle Islands National Lakeshore showing relative coastal change potential. The map is color-coded by potential: High (red), Moderate (orange), Low (yellow), and Very Low (green). The map includes labels for various islands and features, and a legend for the change potential categories.

Figure 3 Glacial Isostatic Adjustment for the Great Lakes.

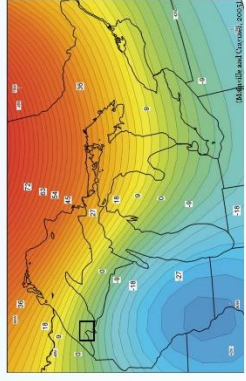


Figure 3 is a map of the Great Lakes region showing glacial isostatic adjustment. The map is color-coded by adjustment: High (red), Moderate (orange), Low (yellow), and Very Low (green). The map includes labels for various lakes and features, and a legend for the adjustment categories.

Method

- Topographic elevations at the Stockton Island Tombolo will be compared with topographic and subsurface elevations at sites of previous researchers reconstructed palaeohydrographs in Lake Superior
- Elevation is collected from Lidar data available through the National Oceanic and Atmospheric Administration
- Lidar data will be of the height of the median dunes, so an estimated subsurface contact (lacustrine deposits) elevation will be used by applying the appropriate correction factor
- First a simple correction developed in Johnston et al. (2012) will be used then other options will be developed
- The ages for the AINL palaeohydrograph will be estimated by comparing the elevations at AINL to other shoreline sites that have palaeohydrographs
- GIA will be applied to account for elevation changes through time caused by the vertical elevation adjustments related to the Laurentian Ice Sheet

Conclusion

Preliminary conclusions about the undergraduate thesis research include:

- The Stockton Island Tombolo probably formed about 6,000 years ago according to peat and charcoal records from the Stockton Island Bog and Lagoons (Huff, 2010)
- Palaeohydrographic research in Lake Superior predicts lake levels are going to be high for several years (Johnston et al., 2012), so the Stockton Island Tombolo and the Pine Barrens Habitat are expected to be in danger from erosion and flooding
- Fieldwork that includes coring shorelines of the Stockton Island Tombolo is planned for Summer 2021. The result from this thesis is expected to help decide the number of cores to collect and where shorelines are cored. The fieldwork will evaluate the methods and interpretations of this thesis
- If proven accurate this topographically corrected method can allow for remote sites to be analysed around Lake Superior, the Great Lakes and beyond

Acknowledgements

I would like to thank Dr. John Johnston for his insight, expertise and editing advice. Emily Secord for helping editing of my work and support throughout this process. Kate Mercer for her help with finding sources. Finally, to my family for all of the support and encouragement they have given to me.

Poster presentation for the finalized thesis.

Remote Paleohydrograph Reconstruction for the Stockton Island Tombolo

Dayna Opersko

University of Waterloo, Department of Earth and Environmental Science

Abstract

Rising lake levels have become a concern for the coasts of Lake Superior and one such coastline is the Stockton Island Tombolo (SIT) that protects the Pine Barrens Habitat (PBH) in the Apostle Islands National Lakeshore (AINL), Wisconsin, U.S.A. (Figure 1). If the SIT is lost, then threatened and endangered species will disappear. For the AINL managers to make an informed decision on how to protect this unique and sensitive site, they need to understand how lake level and sedimentation have changed over time. Paleohydrographs of Lake Superior have been reconstructed from ancient preserved shorelines, creating paleohydrographs that help to understand how lake level has changed in the past by comparing age and elevation (Johnston et al., 2012). Though fieldwork has been postponed due to COVID-19, there is an opportunity here to develop ideas mentioned in Johnston et al. (2012) and Heather (2021) using topographic elevations and a correction factor to reconstruct a paleohydrograph from the ancient shorelines at AINL. Elevations were retrieved from light detection and ranging (LIDAR) data, after a Digital Earth Model (DEM) was created. The DEM was divided into the East and West strandplains and one transect from each was chosen, the two were combined to form the SIT paleohydrograph. Then, elevations were adjusted to estimate the base of the foreshore contact, normally obtained from cores. Trends and patterns in the representative paleohydrograph are compared to paleohydrographs from Johnston et al. (2012) to determine paleohydrograph patterns for the SIT. The paleohydrograph ridges are determined to be from the Nipissing phase while the lakeward ridges are from the Sault phase. This new remote paleohydrograph reconstruction for the SIT helps to preliminarily interpret strandplain sequences in the SIT, potentially helping guide future fieldwork and better understand the context for managing the SIT and PBH in AINL.



Figure 1 Location of Stockton Island Tombolo. The red box indicates the location of the Stockton Island Tombolo (SIT) in the Apostle Islands National Lakeshore (AINL), Wisconsin, U.S.A.

Context

- Studies have been completed at AINL mainly focusing on plants and animals. One coastal study at the SIT showed a very high change potential (Pendleton et al., 2007)
- AINL management plan states sandscapes can go through erosion and deposition. For species on the PBH, the National Park Service mandates to conserve and protect (National Park Service, 2011)
- When many ancient shorelines are preserved strandplains will form and they are composed of ridges that are separated by swales
- A research group has reconstructed lake levels for the past six millennium in the upper Great Lakes with a multi-decadal resolution. One site is near the outlet for Lake Superior in Sault Ste. Marie (SSM). Paleohydrographs have been created from coring through ancient shorelines for past lake level elevation and age dating sediments using OSL. (Johnston et al., 2012 and 2014)
- In Johnston et al. (2012) an idea is mentioned that uses topography and a correction factor to reconstruct an inferred paleohydrograph, further developed by Heather (2021)
- LIDAR is the most detailed and accurate remote sensing data for elevation and can go through most foliage to reconstruct ground surface or topographic elevations (Brook & Purkis, 2009)
- GIA causes vertical elevation changes through time and affect the elevation results and interpretations. GIA rates have been published using geological data from paleohydrographs (Johnston et al., 2012) as well as from water level gauge data (Mainville & Craymer, 2005)

Objectives

- Reconstruct a paleohydrograph with corrected LIDAR elevations and inferred ages for ancient shorelines in the SIT, AINL, adjacent to Lake Superior in Wisconsin, U.S.A.
 - Correct selected LIDAR elevations to best represent past lake level elevations for each ancient shoreline and estimate the millennial lake level phase the ridges formed in
- ## Method
- Elevation is collected from LIDAR data available through the Wisconsin State Geology and AINL. AINL's Digital Coast <https://coast.mn.gov/digitalcoast/data/>
 - LIDAR data is used to create a DEM in ArcGIS to obtain elevations for the ground surface points along transects (Figure 2)
 - Ground surface elevations in swales between beach ridges are corrected to estimate subsurface sedimentary contacts (lucustrine deposits) used to infer lake level elevation
 - Transects for the West and East strandplains were formed to find a representative for each strandplain
 - The West and East strandplains representative transects are compared to find similar elevation trends and patterns needed to create one inferred paleohydrograph pattern for the SIT
 - Different rates of GIA were evaluated by comparing them to paleohydrographs in Lake Superior from Johnston et al. (2012) to the SIT inferred subsurface elevations to estimate age

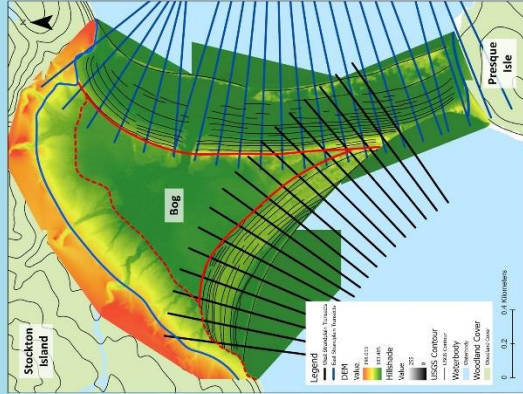


Figure 2 DEM with marked ridges and extent of the tombolo and strandplains. Ridges on both the East and West strandplains have been denoted by the thin black lines. The strandplains have been denoted by solid red lines with the bog meeting between them in the north. The northern extent is seen by solid blue line and dashed red line for a possible closer extent. Solid blue line at Presque Isle is the Southern extent. The thicker black straight lines are the West strandplain transects and the straight blue lines are the East strandplain transects.

Results and Discussion

- Sloping and a bend in the creek on the East strandplain and position among lakeward ridges corresponds to a change in the active outlet for Lake Superior around 1060 years ago or between the Sub-Sault and Sault phases (Johnston et al., 2007, 2012)
- Compared to paleohydrograph data from Johnston et al. (2012) the lakeward (younger) part of the remote paleohydrograph reconstruction for the SIT plotted below all others, fitting with a negative rate of GIA compared to the SSM outlet and estimated to form during the Sub-Sault phase (Mainville and Craymer, 2005; Johnston et al., 2012). The lakeward (oldest) part of the SIT plots above many others suggesting an older age (Figure 3)
- Data from the SIT was plotted with the outlet paleohydrograph for Lake Superior at SSM. The lakeward ridges seem to correlate to the Sub-Sault phase. GIA rate of -15 cm/century appears to correlate best with evidence for the lakeward segment (Figure 4)
- Highest elevation for the Nipissing phase is 183.3m which is similar to the highest peak of the lakeward segment of 184.6m (Thompson et al., 2014)

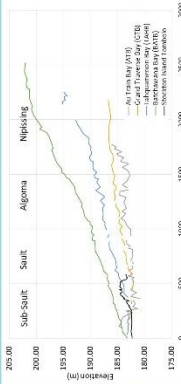


Figure 3 The Stockton Island Tombolo pattern compared to four previously reconstructed paleohydrographs. Comparison of distance versus elevation. Since the GIA is lower for the SIT than the other paleohydrograph locations the lakeward and lakeward SIT parts should both plot under all the curves. The lakeward part is lower in the Sault phase and the lakeward part is only lower in the Nipissing phase.

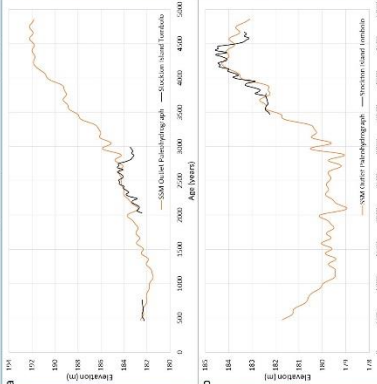


Figure 4 GIA applied to SSM outlet paleohydrograph to compare with the SIT pattern. a) Rate of GIA adjusted by -15 cm/century causing the lakeward and lakeward ridges to be in the Algoma and Sub-Sault phases, respectively. b) Rate of GIA adjusted by -33 cm/century causing the lakeward ridges to be in the Nipissing phase. SSM paleohydrograph data from Johnston et al. (2012)

Results and Discussion

- Lakeward ridges either corresponded to the Algoma (rate of GIA at -15 cm/century) or Nipissing (rate of GIA at -33 cm/century) phases (Figure 4). Since the active outlet during both phases is Port Huron/Sault and the peak Nipissing elevation at this outlet is similar in elevation at a common zero GIA isobase (Mainville and Craymer, 2005; Johnston et al., 2012) then the lakeward SIT segment is estimated to form during the Nipissing phase
- Since the active outlet regulating the water phase in Lake Superior is SSM, there is a continual risk of erosion and flooding at the SIT if the long-term rate of lake-level rise outpaces sediment supply. If sediment supply is faster than the long-term rate of lake level rise then the sediment may protect areas further inland

Conclusion

- The SIT lakeward ridges are estimated to be from the Nipissing phase while the lakeward ridges are estimated to be from the Sub-Sault phase
- The PBH mainly forms on the lakeward ridges, it is protected for now from erosion and flooding
- Paleohydrographic research in Lake Superior predicts lake levels are experiencing a relative rise at the SIT (long term due to GIA and short term due to climate) (Johnston et al., 2012), so the SIT and the PBH are expected to be in danger from future erosion and flooding
- The results from this thesis are expected to help guide fieldwork
- Fieldwork at the SIT can be used to evaluate methods presented in this thesis and potentially show another site, in addition to Heather (2021) where topographic elevation data can be used to reconstruct an inferred paleohydrograph

Acknowledgements

I would like to thank Dr. John Johnston for his insight, expertise and editing advice. Emily Sved for editing of my work and support throughout this process. Kate Moore for her help with fielding resources. Markus Weiland for his help with GIS. Finally, to my family for the support and encouragement they have given to me.

References

Brook, J. C., & Purkis, S. J. (2009). The emerging role of LIDAR remote sensing in natural resource management. *Journal of Coastal Research*, *25*(1), 1-5. doi:10.2199/25153-0913

Heather, M. (2021). *Comparing paleohydrograph reconstructions from subsurface stratigraphy and topography at the Sault Ste. Marie strandplain*. Undergraduate thesis, University of Waterloo, Waterloo, Canada

Johnston, J. W., Anglin, E. P., Thompson, T. A., Baeckle, S. J., Lepper, K., Wilcox, D. A., et al. (2012). A soil-outlet-referenced mill-to-holocene paleohydrograph for Lake Superior constructed from strandplains of beach ridges. *Canadian Journal of Earth Sciences*, *49*(1), 1263-1279. doi:10.1139/cjes-2011-017

Johnston, J. W., Thompson, T. A., & Wilcox, D. A. (2014). Paleohydrographic reconstruction from beach ridges and strandplains of Lake Superior. *Geological Society of America Bulletin*, *126*(1), 21-28. doi:10.1130/B3088222

Johnston, J., Thompson, T., Wilcox, D., & Baeckle, S. (2007). Coastal and sedimentologic evidence for the segmentation of Lake Superior from Lake Michigan and Huron. *Journal of Paleolimnology*, *37*(3), 349-364. doi:10.1007/s10933-006-9032-3

Mainville, A., & Craymer, M. R. (2005). Present-day tilting of the Great Lakes region based on water level gauges. *Geological Society of America Bulletin*, *117*(7), 1070. doi:10.1130/B25392.1

National Park Service. (2011). *General management plan / wilderness document*. National Park Service, U.S. Department of the Interior

Penland, E. A., Thibault, E. K., & Williams, S. J. (2009). *Climatic change potential assessment of the Pine Barrens Habitat, Apostle Islands National Lakeshore to lake-level changes*. Iacono, Wis. U.S. Geological Survey. Retrieved from: <http://pubs.usgs.gov/of/07/P89866/>

Thompson, J. A., Johnston, J. W., & Lepper, K. (2014). *The contemporary elevation of the peak Nipissing phase at outlets of the upper Great Lakes*. Geological Society of America.

Results and Discussion

- Sloping and a bend in the creek on the East strandplain and position among lakeward ridges corresponds to a change in the active outlet for Lake Superior around 1060 years ago or between the Sub-Sault and Sault phases (Johnston et al., 2007, 2012)
- Compared to paleohydrograph data from Johnston et al. (2012) the lakeward (younger) part of the remote paleohydrograph reconstruction for the SIT plotted below all others, fitting with a negative rate of GIA compared to the SSM outlet and estimated to form during the Sub-Sault phase (Mainville and Craymer, 2005; Johnston et al., 2012). The lakeward (oldest) part of the SIT plots above many others suggesting an older age (Figure 3)
- Data from the SIT was plotted with the outlet paleohydrograph for Lake Superior at SSM. The lakeward ridges seem to correlate to the Sub-Sault phase. GIA rate of -15 cm/century appears to correlate best with evidence for the lakeward segment (Figure 4)
- Highest elevation for the Nipissing phase is 183.3m which is similar to the highest peak of the lakeward segment of 184.6m (Thompson et al., 2014)

Conclusion

- The SIT lakeward ridges are estimated to be from the Nipissing phase while the lakeward ridges are estimated to be from the Sub-Sault phase
- The PBH mainly forms on the lakeward ridges, it is protected for now from erosion and flooding
- Paleohydrographic research in Lake Superior predicts lake levels are experiencing a relative rise at the SIT (long term due to GIA and short term due to climate) (Johnston et al., 2012), so the SIT and the PBH are expected to be in danger from future erosion and flooding
- The results from this thesis are expected to help guide fieldwork
- Fieldwork at the SIT can be used to evaluate methods presented in this thesis and potentially show another site, in addition to Heather (2021) where topographic elevation data can be used to reconstruct an inferred paleohydrograph

Acknowledgements

I would like to thank Dr. John Johnston for his insight, expertise and editing advice. Emily Sved for editing of my work and support throughout this process. Kate Moore for her help with fielding resources. Markus Weiland for his help with GIS. Finally, to my family for the support and encouragement they have given to me.

References

Brook, J. C., & Purkis, S. J. (2009). The emerging role of LIDAR remote sensing in natural resource management. *Journal of Coastal Research*, *25*(1), 1-5. doi:10.2199/25153-0913

Heather, M. (2021). *Comparing paleohydrograph reconstructions from subsurface stratigraphy and topography at the Sault Ste. Marie strandplain*. Undergraduate thesis, University of Waterloo, Waterloo, Canada

Johnston, J. W., Anglin, E. P., Thompson, T. A., Baeckle, S. J., Lepper, K., Wilcox, D. A., et al. (2012). A soil-outlet-referenced mill-to-holocene paleohydrograph for Lake Superior constructed from strandplains of beach ridges. *Canadian Journal of Earth Sciences*, *49*(1), 1263-1279. doi:10.1139/cjes-2011-017

Johnston, J. W., Thompson, T. A., & Wilcox, D. A. (2014). Paleohydrographic reconstruction from beach ridges and strandplains of Lake Superior. *Geological Society of America Bulletin*, *126*(1), 21-28. doi:10.1130/B3088222

Johnston, J., Thompson, T., Wilcox, D., & Baeckle, S. (2007). Coastal and sedimentologic evidence for the segmentation of Lake Superior from Lake Michigan and Huron. *Journal of Paleolimnology*, *37*(3), 349-364. doi:10.1007/s10933-006-9032-3

Mainville, A., & Craymer, M. R. (2005). Present-day tilting of the Great Lakes region based on water level gauges. *Geological Society of America Bulletin*, *117*(7), 1070. doi:10.1130/B25392.1

National Park Service. (2011). *General management plan / wilderness document*. National Park Service, U.S. Department of the Interior

Penland, E. A., Thibault, E. K., & Williams, S. J. (2009). *Climatic change potential assessment of the Pine Barrens Habitat, Apostle Islands National Lakeshore to lake-level changes*. Iacono, Wis. U.S. Geological Survey. Retrieved from: <http://pubs.usgs.gov/of/07/P89866/>

Thompson, J. A., Johnston, J. W., & Lepper, K. (2014). *The contemporary elevation of the peak Nipissing phase at outlets of the upper Great Lakes*. Geological Society of America.